



Rapid Detection of Pathogenic Bacteria
using a Silver Enhancement Sandwich Assay

Grant Ongo
Department of Biomedical Engineering
McGill University
August 15, 2014

A thesis submitted to McGill University in partial fulfillment
of the requirements of the degree Master of Engineering.

© Grant Ongo 2014

Table of Contents

Abstract.....	1
Résumé.....	3
Acknowledgements.....	5
1.0 Introduction.....	6
1.1 Motivation.....	6
1.1.1 Hospital Acquired Infections.....	7
1.1.2 Foodborne Illness.....	8
1.2 Bacterial Detection Methods.....	11
1.2.1 Agar Plating.....	11
1.2.2 Polymerase Chain Reaction.....	12
1.2.3 Immunological Methods.....	14
1.2.4 Biosensors.....	16
1.3 Project Rationale.....	17
1.3.1 Binders: Bacteriophage and Antibodies.....	19
1.3.2 Silver Enhancement for Detection.....	21
1.3.3 Low-Cost Optical Detection.....	23
2.0 Materials and Methods.....	25
2.1 Bacteria Culture.....	25
2.2 Bacteriophage Propagation.....	27
2.3 Antibodies against <i>E. coli</i>	29
2.4 Surface Functionalization and Binder Immobilization.....	30
2.5 Microarray Platform.....	32
2.6 Silver Enhancement of Captured <i>E. coli</i>	33
2.7 Fabrication of a Microfluidic Bead Trap.....	34
2.8 Microscopy and Imaging.....	35
3.0 Results and Discussion.....	36
3.1 Bacteriophage Capture of <i>Escherichia coli</i> K-12.....	37
3.1.1 Immobilization of T4 Bacteriophage.....	37
3.1.2 Microcontact Printing of T4 Bacteriophage.....	40
3.1.3 Microarray Printing of T4 Bacteriophage.....	42
3.2 Antibody Capture of <i>Escherichia coli</i> O157:H7.....	47

3.2.1	Optimization of Antibody Immobilization.....	48
3.2.2	<i>Escherichia coli</i> Capture by Antibodies.....	51
3.3	Silver Enhancement for <i>Escherichia coli</i> Detection.....	55
3.4	Microbead Trap for Bacteria Capture.....	62
3.4.1	Microfluidic Bead Trap Design.....	63
3.4.2	<i>E. coli</i> Capture in Bead Traps.....	66
3.4.3	Refractive Index Matching of Microbeads.....	68
3.4.4	Silver Enhancement Assay in Microbead Traps.....	70
4.0	Conclusion.....	73
4.1	Summary.....	74
4.2	Future Work.....	76
	Abbreviations.....	80
	References.....	81

Table of Figures

- Figure 1: E. coli K-12 growth curve for estimation of concentration by optical density measurement.** A) Absorbance of an E. coli K-12 culture at 600 nm over 8 h, progressing through lag, exponential and stationary growth phases. Error bars obtained from triplicate measurements of optical density. B) Curve relating cfu/ml to optical absorbance at 600 nm. CFU/ml estimated from triplicate counts of cfu on agar plates of serial dilutions each hour..... 27
- Figure 2: Specificity of BacTrace® Anti-Escherichia coli O157:H7 antibody from KPL.** Direct ELISA showing high specificity for E. coli O157:H7 (strains from both KPL and ATCC) with low cross reactivity towards other bacteria strains. Data from www.KPL.com BacTrace® Anti-Escherichia coli O157:H7 product page. 29
- Figure 3: Schematic of microarray slide layout for the optimization of antibody and T4 bacteriophage immobilization.** Each slide consists of 16 blocks; block columns were printed at varied pH (7.5 to 9.0, 2 replicates) while rows were printed with different hygroscopic buffers (50% glycerol and 2M betaine + 25% 1,3-butanediol). Each block contained 4 identical arrays with up to 9 by 8 printed spots. Dilutions of phage or antibody concentration were printed along the 9 columns of each array, while replicate spots were printed along the 8 rows. 32
- Figure 4: Fluorescent micrograph showing capture of E. coli K-12 by T4 bacteriophage on reactive aldehyde-coated glass.** A) APTES/glutaraldehyde functionalized surface covalently bound to T4 bacteriophage captures E. coli K-12 compared with B) significantly lower capture on a negative control of APTES/glutaraldehyde-coated glass blocked with BSA. 38
- Figure 5: Variations in the capture of E. coli K-12 by T4 phage immobilized on reactive aldehyde-coated glass.** A) High density of E. coli K-12 capture observed at the edge of wells. Scale bar shows 200 µm. B) Coffee ring effect of captured E. coli K-12 by T4 phage immobilized by a droplet incubated on the surface. Scale bar shows 100 µm. 39
- Figure 6: Microcontact printed T4 bacteriophage on poly-L-lysine-coated glass**

captures stripes of E. coli K-12. A) Fluorescent micrograph of GFP-expressing E. coli K-12 captured by microcontact printed T4 bacteriophage on PLL. Scale bar shows 100 μm . B) Grayscale intensity measurement showing stripes were printed, however the variation of captured E. coli varies significantly..... 42

Figure 7: E. coli K-12 capture by microarray of T4 phage dilutions. Highest capture densities of E. coli K-12 observed at pH 9.0 printed in a 1:1 ratio (see Table 1) with 50% glycerol. Red circles of 150 μm diameter where spots were printed are added for visualization purposes. Phage dilution ratios listed on the left. Data for 1:0 and 0:0 not shown (no capture observed). 44

Figure 8: High titer of spotted T4 bacteriophage capture GFP labeled E. coli K-12 with high density on reactive aldehyde coated surfaces at pH 9.0. A) Xenobind® reactive aldehyde and B) APTES/Glutaraldehyde. Visible streaking of captured cells with the APTES functionalized surface suggests the binding capacity of the surface was exceeded. Scale bar shows 150 μm 45

Figure 9: Effect of printing buffer and pH on the density of captured E. coli by immobilized T4 phage on Xenobind®. 50% glycerol improves the immobilization of T4 phage when compared to 2M betaine/25% 1,2-butanediol at equivalent pH. T4 phage immobilization is improved with pH up to 9.0. Results for pH 7.5 not shown due to insufficient E. coli capture. 46

Figure 10: Optimization of antibody printing conditions. Three surfaces were examined for antibody immobilization: Epoxy, Xenobind® and APTES/Glutaraldehyde. Hygroscopic printing buffers used were 50% glycerol (left) and 2M betaine with 25% 1,3-butanediol (right) using buffer pH values 7.5, 8.0, 8.5, 9.0. Optimal conditions found at blocks of pH 9.0 (shown here). 50

Figure 11: Spotted antibodies capture E. coli O157:H7 with high density and low background. A) Florescent micrograph of E. coli O157:H7 captured by spotted anti-E. coli printed at 100 $\mu\text{g/ml}$ followed by blocking with BSA. Scale bar shows 200 μm . Inset shows magnified view of a single spot with captured E. coli O157:H7. B) Grayscale intensity plot of array showing uniform capture of E. coli cells in spots and comparably low background. 52

Figure 12: Fluorescent image of E. coli O157:H7 patterns captured by anti-O157:H7 antibodies. A microarray of anti-O157:H7 antibodies were printed with 2M betaine and 25% 1,3-butanediol at 100 µg/ml on Xenobind® at pH 9.0, followed by incubation with SYTO® 9 stained E. coli O157:H7. E. Coli were captured in non-homogenous patterns, suggesting a problem with the antibody immobilization..... 53

Figure 13: Fluorescent image showing patterns of captured E. coli O157:H7 results from irregularities in antibody immobilization. A) E. coli O157:H7 stained with SYTO® 9 are captured in the same regions as B) the immobilized antibodies (spiked with Alexa Fluor® 405) printed with 2M betaine +25% 1,3-butanediol (pH 9.0) on Xenobind® C) Merged image of E. coli O157:H7 and antibody distribution. Scale bars show 100 µm. 54

Figure 14: Schematic of a sandwich assay for the detection of bacteria by silver amplification. 1) E. coli is captured from the sample by immobilized capture antibodies specific against the target pathogen. 2) Captured cells are coated with a biotinylated detection antibody. 3) Streptavidin nanogold binds to the detection antibody. 4) Nanogold catalyzes the local reduction of silver..... 56

Figure 15: Dark field micrograph of silver enhanced E. coli O157:H7. A) Silver enhanced E. coli O157:H7 captured by anti-O157:H7 antibody and B) negative control blocked with 2% BSA where no capture is observed. Scale bars show 10 µm. C) low magnification (20x objective) view showing that individual cells are distinguishable. Scale bar shows 50 µm. 58

Figure 16: Carbonate buffer preserves the morphology of E. coli O157:H7 but increases background noise. A) dark and B) bright field micrographs of silver enhanced E. coli O157:H7 using carbonate buffer for washing. C) dark and D) bright field micrographs of negative controls show carbonate buffer also increases background noise by encouraging the spontaneous formation of silver precipitates. Scale bars show 10 µm. 60

Figure 17: Particle counting approach in ImageJ for estimating capture density of E. coli. A) A bright field image is converted to grayscale and B) thresholded to identify cells. C) the image is converted to binary, and using the “Watershed”

algorithm, touching particles are separated by a thin white line (inset). Scale bar shows 10 μm 61

Figure 18: Standard curve for detection of *E. coli* O157:H7 on Xenobind® glass using the silver enhancement assay. A sensitivity of roughly 10^7 cfu/ml was achieved, likely due to multiple washing steps and shear stress during the course of the assay, and the limited surface area available for capture. 62

Figure 19: Microfluidic bead trap sieve designs. Each device consists of two chambers to run the experiment (antibody coated beads) and negative control (BSA coated beads) simultaneously. A) Original bead trap design with 40 μm sieves. Inset shows problematic bead clogging at inlet channels. B) Second version of the bead trap with larger, curved inlet channels to avoid bead clogging, and 37 μm sieves. Inset shows beads being trapped at the sieves. Scale bar shows 2 mm. 64

Figure 20: Microfluidic bead trap packed with PMMA microbeads. Microbeads 38-45 μm in diameter are trapped in place by 37 μm sieve channels, producing a packed bed of microbeads roughly 100 μm in depth. 65

Figure 21: Fluorescent antibody immobilization on carboxylated PMMA microbeads. A) Alexa Fluor® 488 IgG immobilized to carboxylated PMMA microbeads through EDC/NHS coupling compared (1 s exposure) compared with a negative control B) of microbeads first blocked with BSA followed by incubation with Alexa Fluor® 488 (1 s exposure). Inset in B) shows weak fluorescent signal at 10 s exposure, verifying the presence of microbeads. Scale bars show 100 μm 66

Figure 22: Anti-O157:H7 antibody coated PMMA beads capture *E. coli* O157:H7 in a microfluidic bead trap. A) *E. coli* O157:H7 stained with SYTO® 9 are captured on antibody coated beads versus B) a negative control of BSA coated beads. Scale bars show 100 μm . C) Test (left) and adjacent negative control (right) bead chambers. Scale bar shows 1 mm. 67

Figure 23: Time course micrograph of refractive index matching PMMA beads with 64% aqueous ammonium thiocyanate. PMMA beads in water at A) 0 s, being flushed with 64% aqueous NH_4SCN at B) 4 s and C) 8 s. Upon refractive index matching, the beads become virtually invisible. Scale bar shows 1 mm. 70

Figure 24: Dark field images of silver enhanced E. coli O157:H7 is the microbead trap using refractive index matching. A) Capture of E. coli on beads coated with anti-O157:H7 versus B) a negative control of BSA coated beads. Microbeads are clearly visible, and silver enhanced bacteria cannot be observed. C) Silver enhanced bacteria captured by antibody-coated beads becomes visible following refractive index matching with 64% aqueous ammonium thiocyanate. Inset shows what appear to be individual silver coated E. coli O157:H7. D) Negative control following refractive index matching shows low capture of E. coli O157:H7. Scale bars show 50 μm 72

Abstract

Infectious diseases caused by pathogenic and antibiotic-resistant bacteria are a growing problem worldwide. Reliable and high-throughput detection of pathogenic bacteria is an urgent need facing society today. Current diagnostics used to detect bacteria, such as agar plating and real-time PCR, are time consuming, laborious, and often require expensive lab grade equipment. To address the serious need for widespread, inexpensive, and rapid diagnostics, we demonstrate a novel test for the low-cost detection of pathogenic bacteria using a silver enhancement sandwich assay that can be completed in less than 2 h. Using *E. coli* as a model organism, we evaluate T4 bacteriophage against *E. coli* K-12 and antibodies against *E. coli* O157:H7 as potential binders for the capture of bacteria. We optimized the immobilization of binders on different surfaces using a microarray platform and found that both T4 phage suspended in 50% glycerol at high pH (9.0) and antibodies in 2M betaine with 25% 1,3-butanediol at high pH (9.0) immobilized well on reactive aldehyde surfaces. To address several limitations with using phage for detection, antibodies were used in a proof-of-concept assay to detect and enumerate individual *E. coli* O157:H7. In the assay, *E. coli* were captured by anti-O157:H7 antibodies immobilized on reactive aldehyde-coated glass. Next, biotinylated anti-*E. coli* detection antibodies were used to coat the outer cell surface. Streptavidin-nanogold was introduced and bound to detection antibodies. The nanogold catalyzed the local reduction of silver on the cell surface from silver enhancement reagents, allowing individual cells to be imaged and counted, yielding a sensitivity of $\sim 10^7$ cfu/ml on flat glass. To improve sensitivity, a microfluidic device consisting of a packed bed of PMMA microbeads was

used for bacterial capture. To improve imaging of silver coated bacteria within the packed bed, a refractive index matching fluid of 64% aqueous ammonium thiocyanate was used to render PMMA microbeads transparent while silver coated bacteria appeared as bright particles under dark-field microscopy. Using this refractive index matching approach within a packed bed of microbeads, initial results show detection of *E. coli* at 10^4 cfu/ml. While replicate experiments are needed to further quantify this detection scheme, these preliminary findings suggest a simple and rapid approach that could be used in point-of-care diagnostics for the detection of pathogenic bacteria.

Résumé

Les maladies infectieuses causées par des bactéries pathogènes et résistantes aux antibiotiques sont un problème croissant dans le monde entier. La détection infailible à haut débit de bactéries pathogènes est une demande urgente pour la société d'aujourd'hui. Les méthodes diagnostics utilisés actuellement pour détecter les bactéries, tels que les géloses et PCR en temps réel, sont longues, intensives, et souvent nécessitent des équipements de qualité de laboratoire. Pour répondre à la nécessité grave pour un test diagnostic répandu, rapide, et à faible coût, nous démontrons un nouveau test pour la détection abordable, facile, et rapide (< 2 h) de bactéries pathogènes à l'aide d'un essai en sandwich avec des réactifs d'argent qui servent à amplifier le signal. On utilise *E. coli* comme organisme modèle, et on évalue les bactériophage T4 et des anticorps comme liants potentiels pour la capture des bactéries *E. coli* K-12 et *E. coli* O157:H7, respectivement. Nous avons optimisé l'immobilisation de liants sur différentes surfaces en utilisant une plateforme de biopuces et on a trouvé que le phage T4 en suspension dans 50% de glycérol à pH élevé (9.0) et les anticorps dans 2M bétaine avec 25% de 1,3-butanediol à pH élevé (9.0) ont été mieux immobilisés sur des surfaces aldéhyde réactives. Les anticorps ont ensuite été utilisés pour un essai de validation pour détecter et dénombrer les bactéries *E. coli* O157:H7. Celles-ci ont été capturés par les anticorps O157:H7 immobilisés sur la surface de verre couverte d'aldéhyde réactives. Ensuite, des anticorps de détection biotinylé ont été utilisés pour revêtir la surface externe de la cellule, et se lient à la streptavidine-nanogold. Les nanoparticules d'or catalysent la réduction locale de l'argent sur la surface de la cellule à partir de réactifs d'amplification d'argent, ce qui permet aux cellules individuelles d'être imagées et comptées, avec une

sensibilité d'environ 10^7 cfu/ml sur le verre plat. Pour améliorer la sensibilité, un dispositif microfluidique comprenant un lit de microbilles de PMMA a été utilisé pour augmenter la surface disponible pour la capture. Afin de permettre une imagerie de bactéries revêtues d'argent à l'intérieur du lit de microbilles, un fluide avec un indice de réfraction identique au PMMA consistant de 64 % de solution aqueuse de thiocyanate d'ammonium a été utilisé pour rendre les microbilles de PMMA transparentes. En utilisant cette approche d'égalisation d'indice de réfraction au sein d'un lit garni de microbilles, des résultats préliminaires montrent la détection de *E. coli* à 10^4 cfu/ml. Ces résultats préliminaires suggèrent une approche simple et rapide qui pourrait être utilisée dans le diagnostic de point de soins pour la détection de bactéries pathogènes .

Acknowledgements

The success of this research is thanks to the feedback and guidance of my supervisor, Dr. David Juncker. I would like to express my gratitude to Ayokunle Olanrewaju for our stimulating discussions on the point-of-care bacteria detection project, Sebastien Ricoult for his help with microcontact printing, Veronique Laforte for her insight with protein assays and assistance with the microarray platform, and Kate Turner for her moral support and camaraderie. I would like to give a big thank you to Dr. Nathalie Tufenkji for providing the samples of *E. coli* K-12, *E. coli* O157:H7 and T4 bacteriophage that were used during the course of this research. Thanks to Dan Dixon for our discussions on bacteriophage biosensor applications and for his assistance with T4 phage propagation. Also, this research could not have been possible without the support and guidance of the DJ Group, who's collaborative and friendly environment was conducive to furthering this work. Thanks to everyone in the group for their assistance and constant feedback, and for making the time I've spent at McGill both enjoyable and productive.

I acknowledge the Biomedical Engineering Department at McGill University for their financial support through the Recruitment and Excellence Awards, and the GREAT travel award. Thank you to the NSERC-CREATE Integrated Sensors and Systems (ISS) training program for the excellent workshops and lectures that helped to further this research, and for the financial support through the ISS Masters Award. Also, thank you to the NSERC-CREATE Neuroengineering Training Program for the fascinating lectures on neuroengineering which stimulated interest in a side project to this research on surface bound digital nanodot gradients, and for the financial support.

1.0 Introduction

1.1 Motivation

Rapid and reliable high-throughput detection of pathogenic bacteria is an urgent need facing society today. The global rise of antibiotic-resistant bacteria is a burden on health care systems, costing billions in health care costs and leading to thousands of deaths each year. In 2014, the World Health Organization issued a report on the global surveillance of antimicrobial resistance, claiming that “increasingly, governments around the world are beginning to pay attention to a problem so serious that it threatens the achievements of modern medicine. A post-antibiotic era—in which common infections and minor injuries can kill—far from being an apocalyptic fantasy, is instead a very real possibility for the 21st century (WHO, 2014).” This very real threat demands that new, rapid approaches capable of high-throughput screening for antibiotic resistant bacteria be developed to curb a potential pandemic.

When detecting bacteria, microbiologists are often faced with the proverbial ‘needle-in-a-haystack’ problem, dealing with a large and complex sample matrix, often containing very few – if any – pathogens. This results in the need for amplification steps to increase the number of bacteria in a sample prior to detection. While current gold-standard diagnostic techniques (Section 1.2) are typically sensitive and accurate, they are often laborious, time-consuming (1-3 days) and require expensive lab-grade equipment and trained personnel to appropriately handle samples. Consequently, there is high demand for simple diagnostics to quickly detect pathogens so immediate action can be taken to prevent their spread. Two areas in dire need of such diagnostics are in health

care settings, where the spread of hospital acquired infections are a growing problem (Section 1.1.1), and the food industry where improvements to the quality control process are needed (Section 1.1.2).

1.1.1 Hospital Acquired Infections

Hospital acquired infections (HAIs), also known as nosocomial infections, are a growing problem worldwide. In Canada, an estimated 1 in 9 patients admitted to the hospital will contract a HAI, resulting in upwards of \$200-250 million in health care costs and 8,000-12,000 deaths annually (NIDD, 2008). Similarly, in the United States roughly 2 million HAIs cause nearly 100,000 deaths and incur \$4.5 billion in health care costs annually (Reed & Kemmerly, 2009). These bacterial pathogens are often resistant to all but the most powerful antibiotic treatments and require a trial-and-error approach to treatment, beginning with the safest and least expensive options and progressively moving towards harsher – and potentially dangerous – antibiotics, such as protein synthesis inhibitors. The most prevalent HAIs in North America are methicillin-resistant *Staphylococcus aureus* (MRSA), *Clostridium difficile* (*C. diff*), and vancomycin-resistant *Enterococci* (VRE).

MRSA, currently one of the most pervasive HAIs in North America, is especially problematic given that roughly 1% of the population are carriers of ‘community acquired’ MRSA and may not experience symptoms (DeLeo, Otto, Kreiswirth, & Chambers, 2010; NIDD, 2008). These carriers may unknowingly introduce the infection to a hospital setting. Patients who are immune compromised or have open wounds following surgery are then at risk of bacteremia, a blood stream infection associated with mortality rates of 15-60% (Cosgrove et al., 2003). In Canada, the incidence of MRSA infections increased

17-fold between 1995 and 2006; given that the average cost for a single patient diagnosed with MRSA is \$14,000 (NIDD, 2008), this pathogen alone is a major burden on the health care system.

Current methods of diagnosing HAIs involve obtaining a patient sample and pre-culturing the bacteria to amplify the number of cells, followed by detection with real-time PCR or agar plating with antibiotics (often done in tandem to verify results). While these methods are generally accurate, they are time consuming, require skilled personnel and have a limited throughput, resulting in labs being overwhelmed with patient samples. Screening for HAIs is therefore limited to patients scheduled for upcoming surgery, where there is risk of contracting bacteremia. Unfortunately, this practice does not help reduce the spread of HAIs within health care settings. Yet studies have shown that effective screening of health care workers and high risk patients admitted to hospitals not only reduces transmission of HAIs such as MRSA, but also results in net health care savings (Blok et al., 2003; Papia et al., 1999). This suggests that new, low-cost diagnostics to quickly screen health care workers and high-risk patients upon admission could significantly reduce the number of HAIs and associated health care costs.

1.1.2 Foodborne Illness

Gastrointestinal illness caused by contaminated water or food products provides another major motivation for the development of rapid tests for on-site detection of pathogenic bacteria. An estimated 4 million cases of foodborne illness in Canada (Thomas et al., 2013), and 41 million cases in the United States (Scallan, Griffin, Angulo, Tauxe, & Hoekstra, 2011; Scallan, Hoekstra, et al., 2011) occur annually as a result of both fresh and processed food products contaminated with bacteria, parasites or viruses.

In the United States alone, modest estimates calculate the total cost of foodborne illness for the six most prominent bacteria and the most common parasite at \$6.5-35.5 billion annually (Buzby & Roberts, 2009). Of these, the leading cause of hospitalization and death are bacterial pathogens. The most prevalent of these is non-typhoidal *Salmonella*, accounting for roughly 35% of hospitalizations for foodborne illness and 28% of foodborne illness deaths in the United States (Scallan, Hoekstra, et al., 2011). Antimicrobial drug resistance in *Salmonella*, now widespread in developed and developing countries, is a direct consequence of the antibiotic additives given to food-producing animals (Threlfall, 2002). The most common food products implicated with *Salmonella* are eggs and poultry, which are in direct contact with contaminated chickens, however infection has been known to be transmitted through contaminated pork, beef and even fresh fruits and vegetables (Jackson, Griffin, Cole, Walsh, & Chai, 2013).

Similarly, outbreaks of enterohaemorrhagic *Escherichia coli* (*E. coli*) most commonly occur from food commodities in direct or indirect contact with contaminated beef products. Enterohaemorrhagic *E. coli* (EHEC) colonize the intestinal tract of cattle, and can spread to other commodities such as produce, through the contact of cattle excrement with runoff water. EHEC are especially dangerous given that an extremely low number of cells (<100) are capable of transmitting infection (Kaper, Nataro, & Mobley, 2004). The virulence of EHEC stems from 'shiga-like toxins' (Stx1 and Stx2), also known as verotoxins, which are very similar to those produced by *Shigella dysenteriae*. The toxin binds to the glycolipid globotriaosylceramide (Gb3) cell membrane protein and inhibits protein synthesis by cleaving ribosomal RNA (Kaper et al., 2004). These verotoxin producing *E. coli* (VTEC), also known as Shiga-toxin

producing *E. coli* (STEC), are responsible for the majority of *E. coli* outbreaks resulting from food or water contamination. The most prevalent of these in North America is *E. coli* O157:H7, followed by – what are referred to by the U.S. Centers for Disease Control and Prevention as – ‘the big six’ non-O157 VTEC, namely: O26, O45, O103, O111, O121 and O145. Patients infected with VTEC may present with haemorrhagic colitis (bloody diarrhea) and haemolytic uremic syndrome, a potentially life-threatening condition.

There are strict quality control practices in place for monitoring food commodities for possible bacterial contamination at critical points throughout processing. However, with over 200 known food-associated pathogens – and the emergence of new strains that are not routinely screened for – contaminated products sometimes pass through undetected. Moreover, detection is complicated by a complex sample matrix, often containing many grams of dense food material containing few (if any) pathogenic cells amidst a background of non-pathogenic bacteria. Results are needed as quickly as possible to prevent further downstream contamination. Given the quantity of food-products being processed simultaneously, only a limited number of random samples can be feasibly screened, leaving gaps in the quality control process. Detection is traditionally done through a standard plate count of bacteria in a selective media, often with a pre-enrichment step in broth culture to increase the number of cells for detection, requiring an additional 8-24 h before detection can be completed. Despite the simplicity and low-cost of traditional plating, this method lacks sensitivity and is time consuming. Molecular based processes, such as PCR are often preferred for their speed and sensitivity, however pre-enrichment of bacteria is still crucial to obtain sufficient pathogen DNA amidst a

dense sample background (Gracias & McKillip, 2004). While emerging technologies have demonstrated novel and innovative approaches to pathogen detection, their cost and reliability have limited widespread adoption in the food industry. There is an urgent need for diagnostics capable of rapidly screening a large number of samples to improve safety and quality control in the food industry.

1.2 Bacterial Detection Methods

Bacterial detection methods such as conventional agar plating (Section 1.2.1), polymerase chain reaction (Section 1.2.2), and immunoassays (Section 1.2.3) are well established and common practice. However, a large number of alternative approaches exist for bacterial detection, and this is a field of ongoing research in an effort to produce rapid and reliable results. While several overarching biosensor technologies are presented here (Section 1.2.4), emphasis is placed on technologies most relevant to the work presented in this thesis. For an exhaustive list methods for bacterial detection, the interested reader is referred to comprehensive books (Zourab, Elwary, & Turner, 2008) or reviews (Foudeh, Fatanat Didar, Veres, & Tabrizian, 2012; Ivnitski, Abdel-Hamid, Atanasov, & Wilkins, 1999; Lazcka, Del Campo, & Munoz, 2007) on the topic.

1.2.1 Agar Plating

Conventional culturing and plating of bacteria is one of the first established bacterial detection techniques and remains standard practice today. Despite its slow development time from sample to answer, agar plating and modern variations of the approach are widely used for their selectivity and simplicity. Typically, a sample is enriched in liquid culture to amplify the number of cells for 8-24 h, followed by streaking the sample across a plate of agar (e.g. trypticase soy agar) (Gracias & McKillip, 2004).

Selective media containing inhibitors, such as antibiotics, prevent the growth of other bacteria and allow a particular strain to be detected. Commercial products available for common pathogens, such as CHROMagar® or Rainbow Agar®, exhibit a colour change in the presence of the target bacteria to simplify detection. A positive or negative result is usually achieved within 1-3 days. However, certain slow growing pathogens such as *Campylobacter* can take 4-9 days to achieve a negative result and up to 14-16 days to confirm positive results (Brooks et al., 2004). These traditional methods, while suitable for many applications, are by no means rapid. Therefore, alternative approaches with increased speed and sensitivity are often preferred to diagnose HAIs or screen for food-associated pathogens.

1.2.2 Polymerase Chain Reaction

Polymerase chain reaction (PCR) is a well established molecular biology technique in which a target sequence of DNA is amplified many times, producing thousands of copies for detection. DNA primers, complementary to the 3' and 5' ends of the target sequence, are added to the sample with DNA replication enzymes (e.g. Taq polymerase) and nucleotides. Through repeated thermal cycles of heating and cooling (for denaturation, annealing, and elongation), the target sequence – bracketed by the primers – is amplified exponentially. Real-time PCR (also called quantitative PCR) is frequently the method of choice for bacterial detection and diagnostics. In real-time PCR, an increased fluorescence signal is measured in 'real time' as the reaction progresses through the use of DNA probes (complementary to the target sequence) that only fluoresce upon hybridization with copies of the amplified DNA. This allows for the absolute number of copies present in the original sample to be estimated.

PCR is a sensitive technique, requiring only a few copies (or even a single copy) of DNA to be amplified several orders of magnitude. This sensitivity also means that special care must be taken to avoid contamination in the preparation of samples. With real-time PCR, results can usually be obtained within several hours. However, for detection of bacterial pathogens, a pre-enrichment or amplification of cells is normally required to ensure sufficient copy numbers are present in the sample. PCR also requires trained personnel and lab-grade equipment including thermal cyclers, fluorescent detection equipment, and equipment to automate the handling and processing of samples in high-demand settings such as hospitals. This equipment is expensive, and has only a limited throughput, fueling many research efforts towards producing a low-cost, integrated platform PCR for diagnostics.

While PCR is commonly used in clinical setting to diagnose bacterial infections, the technique must be simplified and integrated into an affordable platform for it to reach its full potential as a point-of-care diagnostic. Research has generally focused on the miniaturization of the reaction chamber, often utilizing microfluidics with small sample volumes to increase thermal cycling efficiency (Roper, Easley, & Landers, 2005). Reaction chambers are designed as either (i) stationary, where the entire chamber undergoes thermal cycles similar to traditional PCR, or (ii) continuous flow, where the sample flows repeatedly through distinct temperature zones on-chip to achieve thermal cycling (Park, Zhang, Lin, Wang, & Yang, 2011). Still, challenges remain in integrating each step of the PCR technique, including sample preparation, amplification, and read out. Several groups have reported integrated PCR platforms (Ahmad & Hashsham, 2012; Kaigala et al., 2008; Liu, Li, Greenspoon, Scherer, & Mathies, 2011), and demonstrated

bacterial detection, for example with *Listera monocytogenes* (Cady, Stelick, Kunnavakkam, & Batt, 2005) and *Bacillus subtilis* (Sauer-Budge et al., 2009).

While PCR-based approaches are promising technologies, they still face a number of limitations preventing their widespread adoption. Sample preparation for PCR is crucial; DNA must be extracted from the sample, and contaminants that inhibit the effective amplification of DNA (such as tissue, blood, proteins, lipids, etc.) must be removed (Breadmore et al., 2003). Sample preparation is a major challenge and often increases the complexity of microfluidic devices, especially for PCR-based techniques where multiple liquid handling steps are required to separate DNA from the sample matrix. Furthermore, these integrated PCR platforms still require bulky external equipment for liquid handling, thermal cycling and fluorescence read-out (Park et al., 2011), making it difficult to perform diagnostics at the point-of-care, or achieve high-throughput sample processing.

1.2.3 Immunological Methods

Immunoassays are an established molecular biology technique that determine the presence and concentration of a biological molecule. This is commonly done with the use of enzyme linked immunosorbent assays (ELISA). In a ‘sandwich ELISA’, an immobilized antibody binds specifically to an epitope on a target antigen and captures it from the sample solution. Next, a detection antibody is introduced, and binds to a second epitope on the target antigen. A secondary antibody, linked to an enzyme, then binds to the Fc fragment of the detection antibody and catalyzes a chemical reaction. This produces a colour change, fluorescent marker, or electrochemical signal that can be used for detection.

ELISA is commonly used for the detection of proteins, viruses and bacteria (whole cells, toxins and excreted proteins) in clinical and laboratory settings. For bacterial detection, protein toxins such as the enterotoxins produced by VTEC *E. coli* (Ball, Finlay, Burns, & Mackie, 1994) or *Cholera* (Almeida et al., 1990) are routine antigenic targets. Strain specific proteins expressed on the cell-surface to promote adhesion, as with VTEC *E. coli* (Kaper et al., 2004), or providing antibiotic resistance, as with the mutant penicillin binding protein (PBP-2a) expressed by MRSA (Ubukata, Nonoguchi, Matsushashi, & Konno, 1989), are also common targets for ELISA. Indeed, many pathotypes express unique surface proteins, such *E. coli* where O antigens (e.g. O157, O26, O11, etc.) of the outer lipopolysaccharide (LPS) are common distinguishers of pathogenic strains that can be used for identification (Kaper et al., 2004).

Immunology-based methods also use these strain specific proteins for enrichment. In immunomagnetic separation, magnetic beads conjugated to antibodies capture cells from the sample with high efficiency. This allows bacteria to be concentrated and purified magnetically, eliminating the need for filtration or centrifugation (Qiu, Zhou, Chen, & Lin, 2009). Increasing the interaction of the sample with surfaces conjugated to binders can achieve similar results. Passing the sample through a packed bed of microbeads coated with antibodies has been shown to be an effective method for the immunoseparation and enrichment of *E. coli* O157:H7, with capture efficiencies greater than 91% (Guan, Zhang, Bi, Zhang, & Hao, 2010). Similarly, capture of extremely rare circulating tumor cells (CTCs) from whole blood has been demonstrated with the CTC-Chip: an array of micropillars coated with epithelial cell adhesion marker antibodies, capable of capturing as few as 5 CTCs per ml of blood (Nagrath et al., 2007).

Functionalized cryogels have also been used to provide greater surface area for bacteria capture of *S. aureus* (Ott, Niessner, & Seidel, 2011). Following enrichment of cells using such immune-based capture techniques, traditional ELISA or alternative methods of detection can be carried out more effectively.

1.2.4 Biosensors

While conventional culturing, PCR and ELISA are widely used techniques for the detection of pathogenic bacteria, many alternative biosensing technologies exist. Recent trends with bacterial biosensors are towards miniaturization – reducing sample volumes to the nanoliter range to decrease analysis time, reduce reagent and material costs, and allow for mass production (Lazcka et al., 2007). Such low-cost, miniaturized biosensors would have good potential as diagnostics to be used at the point-of-care (POC), especially in low-resource settings. Biosensors for bacterial detection can be generally grouped into optical biosensors, resonators and electrochemical biosensors.

Optical biosensors are a popular choice for the detection of bacteria, and are commonly based on a fluorescence signal from an ELISA-type assay (Guan et al., 2010). While detection through optical absorption (i.e. from a colour change) is also possible, the small sample volume in microfluidic based biosensors typically results in a poor limit of detection (Mairhofer, Roppert, & Ertl, 2009). Recently, devices based on surface plasmon resonance (SPR) have become of interest for label-free detection of bacteria with high sensitivity (Baccar et al., 2010). In SPR, a change in the resonance condition of light propagating along a surface of immobilized binders (e.g. antibodies) is measured upon binding of an analyte (e.g. bacteria), eliminating the need for subsequent labeling steps. Similarly, changes in the resonant frequency of a quartz-crystal microbalance

(QCM) upon analyte binding has been used in piezoelectric biosensors to detect *Salmonella* (Su & Li, 2005) and *E. coli* (Mao, Yang, Su, & Li, 2006) at concentrations as low as 10^2 cfu/ml. Electrochemical detection is also commonly used in bacterial biosensors by measuring changes in impedance (Lillehoj, Kaplan, He, Shi, & Ho, 2014), current (Gau, Lan, Dunn, Ho, & Woo, 2001), or potential (Zelada-Guillen, Bhosale, Riu, & Rius, 2010). Electrochemical detection provides a rapid, quantitative readout with high sensitivity, but typically requires complicated fabrication procedures that may hinder mass production .

Together, these biosensors represent a shift towards diagnostics that can be used on-site or at the POC, and an effort to eliminate the need for skilled personnel or lab-grade equipment. While focus has largely been on miniaturization, the small sample volumes used creates an important challenge – they contain few, if any cells. This generally results in the need for amplification of cells through pre-culturing or cell enrichment using immunological based methods.

1.3 Project Rationale

While advances have recently been made in the field of pathogen detection, there is still a general need for simple and sensitive low-cost diagnostic approaches. The goal of this research is to develop a novel detection scheme for the rapid detection of pathogenic bacteria using a silver enhancement sandwich assay with optical detection. The detection scheme should be well-suited for integration into a low-cost, disposable POC diagnostic. Here, our intended application is to detect antibiotic resistant bacteria in clinical settings. Given this, we propose to develop a self-powered capillary microfluidic system to perform a silver enhancement sandwich assay to detect antibiotic resistant

bacteria. The need for external equipment or power supply could feasibly be eliminated using microfluidic circuits based on capillaries to run the assay autonomously (Safaviéh & Juncker, 2013). The assay reagents could be preloaded into the microfluidic chip, and released sequentially after sample delivery to complete the assay without the need for external power. Such a device would have potential in clinical settings as a method to screen health care workers and patients admitted to the hospital for HAIs, allowing immediate action to be taken in preventing the spread of infection.

This research will focus on development and characterization of a silver enhancement-based sandwich assay for the rapid detection of whole cells of pathogenic bacteria. A proof-of-principle assay on glass slides will be demonstrated, and then integrated into a microfluidic device. In addition, the optical detection scheme will be optimized using an index-matching strategy to improve the limit of detection.

We aim to develop a device for rapid screening of patient samples. For this application, the device needs to be rapid and sensitive to provide an initial risk assessment. If necessary, results can be confirmed with a gold-standard test such as PCR. A proof-of concept assay will be developed and characterized using *E. coli* as a model organism, however the strategies outlined will be widely applicable to other bacterial pathogens where affinity binders that target cell surface markers are available. This is feasible for pathogens of interest like *E. coli* O157:H7 and MRSA that have antibodies and bacteriophages against cell membrane proteins.

The proposed mechanism of detection will be to specifically capture *E. coli* cells, and coat them with a layer of reduced silver using silver enhancement reagents in an ELISA-type sandwich assay. Binders for the specific capture of the target pathogen,

including bacteriophage and antibodies (Section 1.3.1) will be investigated. A packed bed of microbeads will be investigated to provide high-surface area for bacteria capture. Following capture, a detection binder will coat the outer cell surface, and catalyze the local reduction of silver from enhancement reagents (Section 1.3.2). Using low-cost optical imaging approaches (Section 1.3.3), detection of pathogens could be achieved. At high concentrations of bacteria, the silver coated cells should allow for a net absorbance value to be measured. When cells are in low concentration, discrete silver-coated particles may be counted. This could potentially reduce or even eliminate the need for an enrichment or amplification step commonly done with current bacteria detection platforms.

1.3.1 Binders: Bacteriophage and Antibodies

Binders are biomolecules with an affinity and specificity for a given target. Commonly used binders for ELISA or other biosensing applications include antibodies, oligonucleotides, aptamers, or even viruses. For example, bacteriophage (phage) are viruses that offer specificity for a ‘host’ bacteria through receptors that target strain-specific surface antigens. Phage are typically isolated from natural environments where bacteria are prevalent, such as sewage water, marine water and soil. Phage coevolve in an evolutionary arms race with their host bacteria, changing their receptor binding proteins (RBPs) to maintain specificity (Koskella & Meaden, 2013). This allows phage to specifically bind to their host and infect it with viral DNA or RNA, inducing replication through either a lysogenic or lytic cycle using the cell’s resources. In the lytic cycle, this ultimately results in the destruction of the host cell through lysis, releasing the newly formed viral particles. This property, unique to lytic phage, offers potential as a means of

signal amplification through the downstream detection of reproduced viruses (Oliveira, Almeida, Hofer, & Almeida, 2012). The affinity for a target host makes phage useful as probes for a multitude of biosensing applications (Singh, Arutyunov, Szymanski, & Evoy, 2012), as a coating to prevent formation of biofilms in clinical settings (Donlan, 2009), and even as an alternative to antibiotics with so-called ‘phage therapy’ (Carlton, 1999).

In biosensors for pathogen detection, phage are immobilized to a surface through physical adsorption, covalent linkage, or genetic modification (i.e. to express biotin). Immobilized phage have been used for the detection of bacteria by quartz-crystal microbalance (QCM), SPR, microcantilever, amperometry, bioluminescence and magnetoelastic platforms (Singh et al., 2012). It is also possible to tag phage with a moiety such as biotin allowing them to be used for subsequent detection steps (Edgar et al., 2006). In the investigation of phage for biosensing applications, T4 phage is often used as a model organism since it is well-characterized. T4 phage possess receptors that target the outer membrane protein C (OmpC) and antigens of the LPS layer on the cell wall of the *E. coli* K-12 strain (Yu & Mizushima, 1982). Here, we will examine phage as a potential binder for use in a silver enhancement assay using T4 phage and *E. coli* K-12.

Antibodies are another commonly used binder for pathogen detection. Unlike phage, where specificity for a target pathogen is typically isolated from a natural source, antibodies can often be readily produced for a given target. Polyclonal antibodies are typically produced by invoking an immune response in a laboratory animal, such as a mouse or rabbit. The animal is inoculated with an inactivated pathogen (or specific antigens) to produce an immune response, and the antibodies produced are isolated from

the serum and purified (Hanly, Artwohl, & Bennett, 1995). These can then be functionalized with moieties for further detection steps, such as biotin or horse radish peroxidase (HRP). For monoclonal antibodies (i.e. targeting a single antigen epitope), a single B lymphocyte producing the antibody is isolated from the immunized animal. This is fused with a myeloma (cancer) cell to generate a hybridoma, an immortal cell line for antibody production (Birch & Racher, 2006). Many polyclonal and monoclonal antibodies against common pathogens already exist, and have been demonstrated as effective binders for bacteria detection through standard ELISA kits, and more specialized biosensors as previously discussed. Here, antibodies against *E. coli* O157:H7 will be investigated as binders for both the capture and detection of *E. coli* O157:H7 using a silver enhancement based sandwich assay.

1.3.2 Silver Enhancement for Detection

Bacteria detection will be achieved by coating captured cells with a layer of reduced silver using silver enhancement reagents, allowing them to be imaged without fluorescent microscopy and with low-cost imaging equipment. Immunogold silver staining has been used in histology as a means of staining tissue samples (Merker, 1983). The technique has also been known to stain plant bacteria, allowing them to be identified under bright field microscopy (Van Laere, De Wael, & De Mey, 1985). However, the general approach has more recently gained attention as a means of signal amplification for detection in biosensors. This is done using a probe (e.g. antibody, oligonucleotide, etc.) targeted to a specific analyte that is conjugated to a gold nanoparticle. The probe, bound to the target analyte, is then exposed to silver enhancement reagents. These reagents contain a silver salt, often silver nitrate, and a reducing agent, such as

hydroquinone (Danscher & Rytter Norgaard, 1985). During development with the enhancement reagents, the nanogold acts as a catalytic site for the reduction of silver, increasing the size of the nanoparticles to the micron range where they appear optically dark. This amplification of the signal allows for detection either optically or through changes in conductance.

Ultra-sensitive optical detection using silver enhancement has been demonstrated with prostate specific antigen at a concentration of 30 attomolar using an inexpensive flatbed scanner to measure colorimetric changes (Nam, Thaxton, & Mirkin, 2003). Similarly, detection of PCR-amplified bacterial DNA has been shown to be observable by eye, and quantifiable using a flatbed scanner (Yeh, Chang, Lin, Chang, & Lin, 2012). The strategy has also been integrated into microfluidic chips to run diagnostic tests at the POC. The 'mChip' uses an ELISA-type assay for the detection of HIV, hepatitis and syphilis using a simple absorbance measurement following silver enhancement; field tests of hundreds of human samples in Rwanda showed diagnostic sensitivities and specificities on par with laboratory results (Chin et al., 2011). Such works demonstrate that silver enhancement is well-suited for highly sensitive, low-cost diagnostics that can be used at the POC.

Here, we will demonstrate detection of whole cells of pathogenic *E. coli* using an ELISA-type silver enhancement assay. It is hypothesized that at high concentrations of bacteria, a net absorbance value – as previously demonstrated – would be measurable. However, by performing the assay on whole cells, individual bacteria may be counted at low bacteria concentrations, as is commonly the case with the original sample. This may lower the threshold concentration needed, as discrete particles could be detected. This

might allow for a reduction or even elimination of the pre-culturing step that is commonly done to amplify the number of cells for pathogenic bacteria detection.

1.3.3 Low-Cost Optical Detection

Advances in camera and optical sensor technology make inexpensive imaging equipment such as USB microscopes, flatbed scanners, and smartphones potential options for quantifiable optical detection of pathogenic bacteria. Leaving behind lab-grade equipment including high-powered microscopes is an important step in making truly POC diagnostics, especially for low-resource settings in developing countries. While this in and of itself is a field of ongoing research and development, many diagnostic tests have already demonstrated they can be used with simple, low-cost imaging equipment or even by the naked eye.

Light emitting diodes (LEDs) have a low-power consumption and unit cost, making them an inexpensive alternative to conventional lasers for fluorescent detection schemes. LED-based fluorescent microscopes have been used to visualize *M. tuberculosis* from patient sputum smears (Albert et al., 2010; Bonnet et al., 2011). More recently, pathogenic *E. coli* and *Salmonella* labeled with quantum dots were detectable at concentrations of 5-10 cfu/ml (in buffer and milk) using a smartphone camera with LED illumination (Zhu, Sikora, & Ozcan, 2012). Optical absorbance measurements from silver enhancement is also a highly sensitive means of detection and is well suited for POC diagnostics. Quantifiable read-out has been demonstrated using flatbed scanners and handheld devices (Chin et al., 2011; Nam et al., 2003). These net measurements of optical absorbance are desirable for POC diagnostics since they do not require high-powered microscopes for detection.

However, recent advances in optical techniques are allowing for increasingly compact and cost-effective imaging at high resolution (Zhu, Isikman, Mudanyali, Greenbaum, & Ozcan, 2013). Lens-free computational imaging techniques, where images are reconstructed in post-processing offer one potential strategy for POC diagnostics. Since an objective lens is not used, methods such as lens-free holography can sample a large field-of-view (24-30 mm²) at sub-micron resolution, making it possible to quickly analyze large sample volumes for particles (Wei et al., 2013). Such advances in imaging techniques make particle counting of silver enhanced bacteria, as proposed here, a feasible method for detection at low concentration. These low-cost imaging methods will be explored as approaches for the detection of bacteria through the silver enhancement assay.

2.0 Materials and Methods

2.1 Bacteria Culture

The common lab strain *E. coli* K-12 was used for experiments with T4 bacteriophage. *E. coli* K-12 strain was transformed with a plasmid for ampicillin resistance and expression of green fluorescent protein (GFP) for visualization by fluorescent microscopy (excitation at 395 nm and emission at 509 nm). An attenuated strain of the pathogenic *E. coli* O157:H7 (ATCC 700728) was used in experiments with antibodies for capture and detection.

Lysogeny broth (LB) for liquid culture was prepared from LB powder (Sigma-Aldrich) at 20 g/L with Milli-Q water. Agar plates were prepared from LB broth powder at 20 g/L, bacteriological agar (Sigma-Aldrich) at 15 g/L and Milli-Q water. LB and agar solutions were autoclaved (Steris SI-120 Scientific Isothermal Sterilizer) on liquid cycle for 45 min (124°C, 18 psi). For culturing *E. coli* K-12, ampicillin (Sigma-Aldrich) was added to LB or agar after autoclaving to a final concentration of 100 µg/ml to prevent growth of other bacteria and induce expression of GFP. For liquid culture, 3 ml volumes of LB were aliquoted into sterile 14 ml polypropylene round-bottom tubes (BD Falcon) and stored at 4°C. Agar plates were poured to a thickness of roughly 5 mm in 60 mm diameter petri dishes (Sigma-Aldrich). Plates were inverted and allowed to dry for 1-2 days, then wrapped in plastic and stored at 4°C.

Frozen aliquots of *E. coli* K-12 and O157:H7 were produced from single colonies selected from streaked agar plate samples. A liquid phase culture from a single colony was grown to exponential phase. Sterilized glycerol was added to a final concentration of

15% (v/v), and the solution was aliquoted in 1 ml cryogenic vials (VWR), flash-frozen in liquid nitrogen, and stored at -80°C. A flame-sterilized inoculating loop (Decon LeLoop; medium, non-calibrated) was scraped along the surface of frozen aliquots to inoculate subsequent liquid cultures or streak agar plates. Inoculated liquid cultures were incubated at 37°C and 200 rpm (Forma Scientific, Orbital Shaker) overnight; agar plates were inverted and incubated at 37°C overnight (Revolutionary Science, RS-IF-203 Incufridge). 50 µl of overnight liquid cultures were used to inoculate 3 ml of fresh LB broth, which was grown at 37°C and 200 rpm for 3-5 h before use. Cultures were transferred to autoclaved 1.5 ml microcentrifuge tubes (Fisher Scientific) and centrifuged (VWR, Galaxy Mini) for 3-4 min at 6000 rpm (2000×g), and rinsed twice with fresh LB broth before use.

For fluorescent microscopy, *E. coli* O157:H7 was stained with SYTO® 9 green fluorescent (excitation at 485 nm, emission at 498 nm) nucleic acid stain (Life Technologies). SYTO® 9 was added to washed cultures to a final concentration of 5 µM and incubated for 30 min, followed by washing 3 times with LB broth.

To estimate the concentration of bacteria cultures in colony forming units per ml (cfu/ml), growth curves were produced. The optical density (OD) of cultures was related to the cfu/ml determined from agar plating of 10-fold serial dilutions. OD was measured (3 replicate measurements) at 600 nm (NanoDrop ND-1000 Spectrophotometer) over 8 h, until cultures had progressed to an apparent stationary phase for 1 h. Each hour, a 20 µl sample of culture was added to 180 µl of fresh LB broth and immediately diluted 10-fold (i.e. 20 µl in 180 µl) 8 times. 10 µl of each serial dilution was spotted on agar plates (3 plates for standard deviation measurements), which were incubated overnight at 37°C.

Dilutions where colonies were countable were used to relate OD to cfu/ml (Fig. 1). While OD was used as an initial estimation of bacteria concentration, agar plating was used to verify concentration (i.e. number of colony forming bacteria) when appropriate.

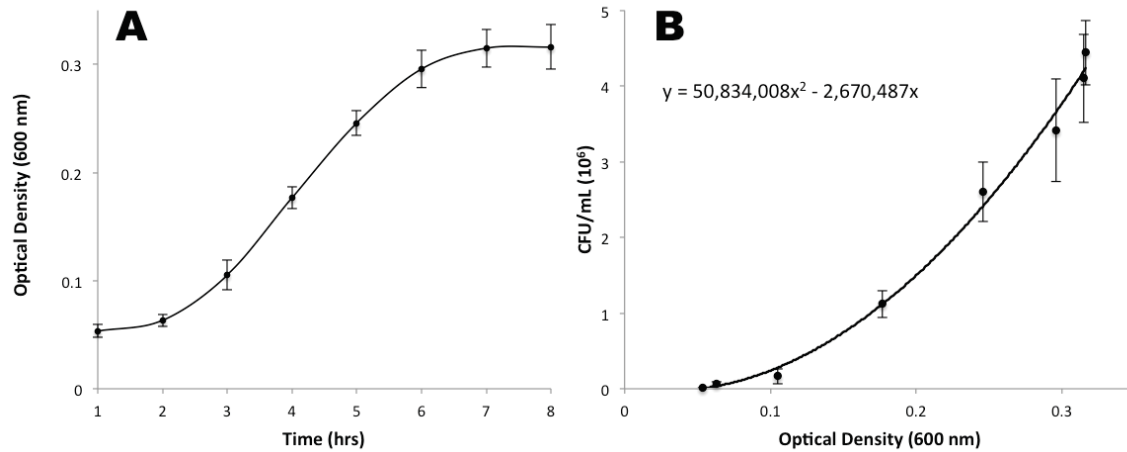


Figure 1: *E. coli* K-12 growth curve for estimation of concentration by optical density measurement. A) Absorbance of an *E. coli* K-12 culture at 600 nm over 8 h, progressing through lag, exponential and stationary growth phases. Error bars obtained from triplicate measurements of optical density. B) Curve relating cfu/ml to optical absorbance at 600 nm. CFU/ml estimated from triplicate counts of cfu on agar plates of serial dilutions each hour.

2.2 Bacteriophage Propagation

T4 bacteriophage were isolated in high titer using a liquid phase propagation method. 5 ml of LB broth was inoculated with 50 μ l of *E. coli* K-12 overnight culture, and incubated at 37°C and 200 rpm for roughly 3 h to reach exponential phase (OD of \sim 0.2). 100 μ l of T4 phage stock (10^9 pfu/ml in SMG buffer) was added to the 3 h culture, and incubation was continued for roughly 5 h. Turbidity decreased significantly as the bacteria were lysed. The culture was removed from incubation and centrifuged for 5 min at 3300 \times g to spin down remaining bacteria and debris, which was discarded. The supernatant containing propagated T4 phage was added to 10 ml of fresh 3 h culture of *E.*

coli K-12, and incubated for roughly 5 h. This was repeated, with increasingly larger volumes of K-12 culture, until 400 ml of lysate was obtained. The solution was cooled to room temperature. DNase I and RNase (Sigma-Aldrich) were added to a final concentration of 1 µg/ml each and incubated for 30 min. NaCl (Sigma-Aldrich) was added to a final concentration of 1 M by continuous mixing for 1 h. The phage suspension was then stored on ice for 1 h. The solution was centrifuged at 3300×g for 10 min at 4°C to remove debris.

The bacteriophage were purified by PEG precipitation (Sambrook & Russell, 2001). 10% w/v PEG (8000 MW, Sigma-Aldrich) was dissolved in the lysate slowly by gradual addition with continuous stirring. The solution was transferred to polypropylene centrifuge bottles and left undisturbed for 3 h on ice to precipitate PEG/phage. The solution was centrifuged at 11,000×g for 1 h at 4°C, leaving a thin white film after decanting the supernatant. This was gently re-dissolved in 60 ml SMG buffer by placing the centrifuge bottles on a rocking platform at 4°C for two days. The re-suspended solution was purified twice using Amicon Ultra-15 centrifugal filters (Millipore) at 4000×g for 1 h (100 kDa membrane NMWL).

The phage titer was determined using the soft agar overlay method (Clokier & Kropinski, 2009). LB broth (20 g/L) with 5 g/L of bacteriological agar was autoclaved in 3 ml volumes. The soft agar was first brought to a boil to remove crystalline solids, then maintained at roughly 50°C in a hot water bath. A series of nine 1 ml 10-fold phage dilutions were prepared in SMG buffer. 100 µl of phage dilution and 100 µl of overnight *E. coli* K-12 culture were added to each aliquot of soft agar, mixed and poured over an agar plate. The soft agar was allowed to cool for 30 min, then inverted and incubated at

37°C for roughly 16 h. A plate with a countable number of plaques (~300) was used to estimate the phage titer. Final titers up to roughly 7×10^{12} pfu/ml were obtained.

2.3 Antibodies against *E. coli*

Antibodies were tested as an alternative to bacteriophage for the capture and detection of *E. coli* O157:H7. Affinity-purified polyclonal antibodies (goat IgG) against *E. coli* O157:H7 were obtained from KPL (Cat. # 01-95-90), offering low cross-reactivity with other common bacteria strains including *E. coli* K-12 and STEC (Fig. 2). Anti-O157:H7 antibodies target antigens on the outer cell surface, including O157 antigen of the LPS and the flagellar H7 antigen. Lyophilized antibodies were rehydrated in 50% glycerol at a concentration of 1 mg/ml, aliquoted in 50 µl volumes and stored at 4°C (for up to 1 year). Anti-O157:H7 antibodies were immobilized on various surfaces by physisorption or covalent bonding for the capture of *E. coli* O157:H7 from solution.

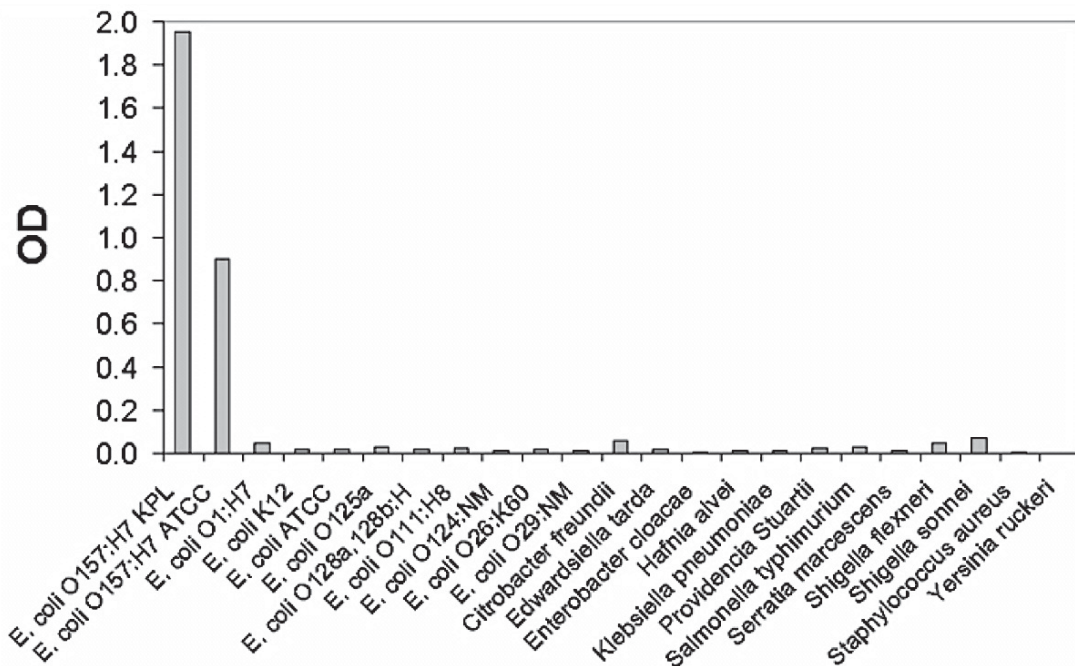


Figure 2: Specificity of BacTrace® Anti-Escherichia coli O157:H7 antibody from KPL. Direct ELISA showing high specificity for *E. coli* O157:H7 (strains from both KPL

and ATCC) with low cross reactivity towards other bacteria strains. Data from www.KPL.com BacTrace® Anti-*Escherichia coli* O157:H7 product page.

Polyclonal anti-*E. coli* antibodies (Abcam, ab68451) against O and K antigenic serotypes (rabbit IgG) were chosen for the detection of *E. coli*. Antibodies were aliquoted at 4.5 mg/ml in PBS (Sigma-Aldrich) at 2 µl volumes and stored at -80°C. These anti-*E. coli* antibodies were used for detection following capture to coat the outer surface of the cell. Antibodies were obtained biotinylated to take advantage of biotin-streptavidin binding in subsequent detection steps.

2.4 Surface Functionalization and Binder Immobilization

Surfaces were functionalized to facilitate the immobilization of bacteriophage and antibodies for *E. coli* capture. For covalent linkage, a reactive aldehyde coating on glass was produced. Slides were first plasma activated for 60 s with air plasma (PE-50 HF, PlasmaEtch: 150 mTorr, 13.56 MHz, 300 W) to clean the surface and produce reactive hydroxyl groups for silanization. Slides were then placed under vacuum in a silane chamber (Belart Space Saver Vacuum Desiccator, 190 mm) at room temperature with several drops of (3-Aminopropyl)triethoxysilane (APTES) for 30 min. The silane end of APTES covalently binds to the glass surface, leaving the tail end with amino group functionality pointing outward. The amino-coated surface was then reacted with 5% glutaraldehyde in DI water for 1 h, and rinsed with PBS, resulting in reactive aldehydes for phage and antibody immobilization under basic conditions.

Poly-L-lysine (PLL) coated glass was used in physisorption experiments. Glass slides were plasma activated for 60s, then immersed in a solution of 0.01% PLL and

placed on a rocker for 10 min to evenly coat the surface. The solution was aspirated, and slides were dried for at least 2 h before use.

Other pre-functionalized surfaces tested for phage or antibody immobilization include epoxy and aldehyde coated surfaces. Nexterion® Slide E glass slides (Schott, Germany) coated with an epoxy-silane allow for reproducible, high density (3.7×10^{12} molecules/cm²) covalent linkage of proteins or other probes possessing amino groups (Xing & Borguet, 2007). Similarly, Xenobind® glass slides (Xenopore, USA) coated with a reactive aldehyde irreversibly and covalently bind to proteins or amino containing molecules at a density of roughly 250 ng/cm² claimed for IgGs (xenopore.com/products/xenobind).

For immobilization of antibodies on microbeads, poly(methyl methacrylate) (PMMA) microbeads (38-45 µm diameter, Cospheric, USA) were selected for their low refractive index ($n_D = 1.489$). However, PMMA does not naturally possess reactive surface groups and must first be functionalized to allow for the immobilization of antibodies. PMMA beads were carboxylated through an acid catalyzed hydrolysis (Toh, Wang, & Ng, 2008). PMMA beads were activated with 1M sulfuric acid under continuous stirring for 20 min at 60°C, followed by thorough rinsing with DI water, resulting in a surface functionalized with carboxylic acid groups. Carboxylated microbeads were then coupled to antibodies through EDC/NHS coupling. A 1 ml 10% (w/v) suspension of carboxylated microbeads was incubated with EDC (50 mM) and NHS (50 mM) in MES buffer for 20 min, followed by rinsing with MES. Antibodies were coupled to EDC/NHS activated beads by incubating for 2 h at concentrations of 0.1-0.4 mg/ml.

2.5 Microarray Platform

Conditions for immobilization of phage and antibodies on various surfaces were optimized using a microarray platform. Variables such as the printing buffers, concentration, and pH range were examined on the same surface simultaneously, reducing variation across experiments and providing replicate spots for reproducibility. A Nanoplotter 2.0 inkjet spotter (GeSiM, Germany) was used to deposit nanoliter volume droplets of phage or antibody solutions on the surface of a functionalized glass slide. The slide layout consisted of 16 blocks of phage or antibody dilutions printed under different pH and printing buffer conditions (Fig. 3).

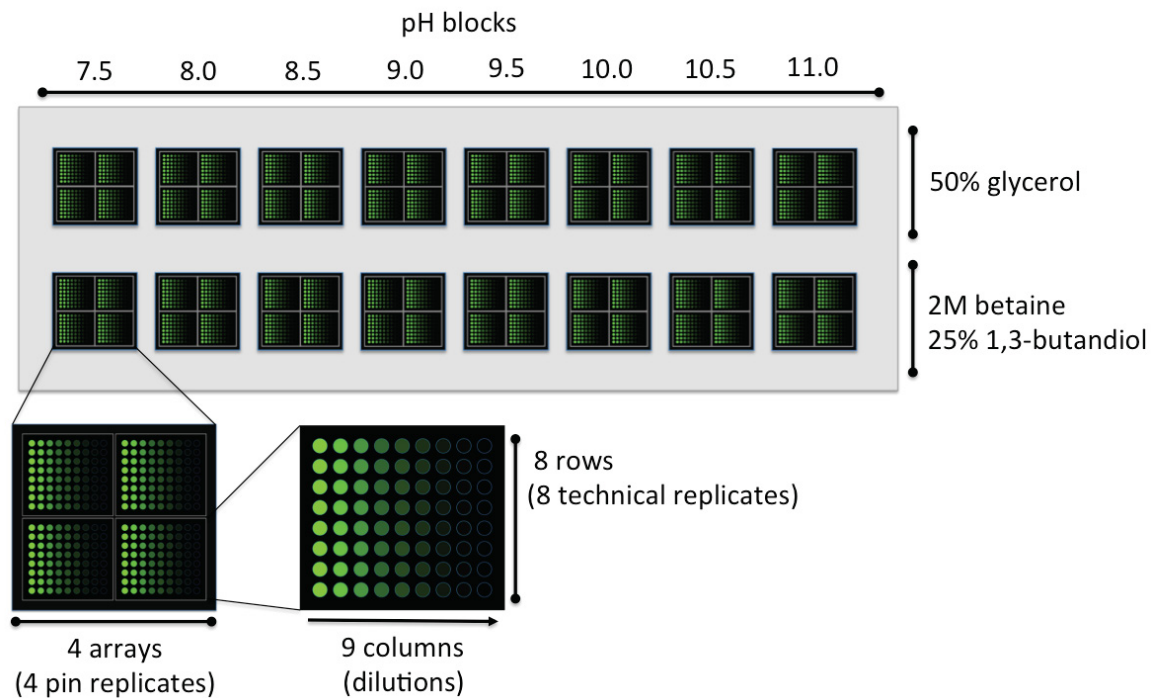


Figure 3: Schematic of microarray slide layout for the optimization of antibody and T4 bacteriophage immobilization. Each slide consists of 16 blocks; block columns were printed at varied pH (7.5 to 9.0, 2 replicates) while rows were printed with different hygroscopic buffers (50% glycerol and 2M betaine + 25% 1,3-butanediol). Each block contained 4 identical arrays with up to 9 by 8 printed spots. Dilutions of phage or antibody concentration were printed along the 9 columns of each array, while replicate spots were printed along the 8 rows.

Phage and antibody dilutions were prepared in printing buffers at varied pH to be spotted. A range of basic pH values from 7.5 to 9.0 was selected to facilitate binding to reactive aldehyde and epoxy coated surfaces. Two printing buffers for microarrays were selected; 50% glycerol and 2M betaine with 25% 1,3-butanediol. 50% glycerol is a common printing buffer used in protein microarrays, since it is hygroscopic, and improves spot morphology and efficiency of binding on reactive aldehyde surfaces (Olle et al., 2005). A second buffer containing 2M betaine as a hygroscopic agent and 1,3-butanediol as a solvent was tested given its recent demonstration as an effective low-evaporation additive for antibody immobilization in protein microarrays (Bergeron, Laforte, Lo, Li, & Juncker, 2014).

Following printing, slides were placed in a humidified chamber (60% relative humidity) to reduce evaporation, and allowed to react overnight. 16-well silicone gaskets (Grace Bio-Labs, USA) were used to separate blocks of different printing conditions. Wells were incubated with 2% BSA in PBS for 2-3 h to block the non-printed surface, followed by rinsing with PBS (×3) at 200 rpm for 5 min (Thermo-Shaker, BioInstruments) prior to use.

2.6 Silver Enhancement of Captured *E. coli*

Silver enhancement of captured *E. coli* was used as a method to coat bacteria with a layer of reduced silver, allowing them to be easily visualized without the need for fluorescent microscopy. Following capture of *E. coli* O157:H7 with anti-O157:H7, and detection with biotinylated anti-*E. coli*, a 100× dilution of streptavidin-nanogold (Nanoprobes) in PBS was incubated with cells for 30 min, followed by rinsing

thoroughly with DI water. Silver enhancement solutions generally consist of two solutions; Solution A contains a silver salt, typically silver nitrate (AgNO_3), and Solution B contains a reducing agent, normally hydroquinone in addition to stabilizers such as glycerol to prevent spontaneous silver reduction (Danscher & Rytter Norgaard, 1985). Silver-enhancement reagents (Sigma-Aldrich) were mixed in equal ratios at room temperature immediately before use. Following mixing, the solutions were stable for 20-30 min. An optimal developing time of 5 min was determined by experiment to coat cells sufficiently with a layer of reduced silver, while limiting the formation of background silver precipitates. After silver development, samples were washed thoroughly with DI water, and imaged by dark or bright field microscopy.

2.7 Fabrication of a Microfluidic Bead Trap

A microfluidic ‘bead trap’ was designed to capture beads in place using a sieve of channels slightly smaller than the diameter of microbeads selected. A single layer mask design was produced in L-Edit layout editing software (Tanner EDA) and a 5 μm resolution chrome photomask was fabricated (Front Range PhotoMask). An SU-8 master of 100 μm in depth was patterned on a 7” silicon wafer (University Wafer) by photolithography in the McGill Nanotools clean room facilities. The SU-8 master was used to produce inverse replicas in polydimethylsiloxane (PDMS). Prior to producing replicas, the SU-8 master was plasma activated for 60 s, and silanized with 1H,1H,2H,2H-Perfluorooctyltriethoxysilane (Sigma-Aldrich) by vapor deposition to prevent adhesion of PDMS following curing. After silanization, many PDMS replicas can be generated from the master.

PDMS monomer was mixed thoroughly with initiator in a 10:1 ratio (Dow Corning) and poured on the master wafer. The wafer was degassed under vacuum to remove bubbles from the PDMS, and cured at 60°C overnight. After removal of the PDMS replica from the wafer, devices were cut out and sonicated in 70% ethanol for 2 h to remove extractables (unreacted monomer and silicone oils). Prior to use, holes were punched at the inlets and outlets, and tape was applied to the device to remove any particulates. The device and a glass slide were plasma activated for 60 s, then brought into contact and left for 20 min to facilitate bonding, resulting in a watertight seal. 1/16 inch polymer tubing (TFL FEPTB 1/16IN OD0.30 ID20, Fisher Scientific) was inserted into inlets and outlets, and threaded into syringe adapters (IDEX Health & Science) to connect with syringes loaded with assay reagents.

Prior to use, bead chambers were packed with a 1% suspension of PMMA beads pre-immobilized to anti-O157:H7 antibodies prior to use. 1 ml syringes (BD Falcon) pre-loaded with bacteria culture or assay reagents were connected to adapters as necessary, and loaded into a dual infusion/withdrawal syringe pump (Model 200, KdScientific) to control flow rate to the bead chambers.

2.8 Microscopy and Imaging

Fluorescent images of GFP-expressing *E. coli* K-12 and SYTO® 9 stained *E. coli* O157:H7 were taken with a Nikon TE2000-E inverted microscope using NIS-Elements Advanced Research software suite V2.3 (Nikon). An Xcite 120 (Exfo) laser illumination source was used with a B-2A filter cube (Nikon, blue excitation 450-490 nm, dichromatic mirror 505 nm, barrier filter 520 nm). For experiments involving bacteria capture on flat glass surfaces, a drop of Fluoromount™ aqueous mounting medium (Sigma-Aldrich) was

applied to the surface, covered with a glass coverslip and inverted for imaging. For capture of *E. coli* in bead traps, imaging was done through the glass slide.

Antibody immobilization on glass slides was imaged using an Agilent scanner. Biotinylated antibodies were first spotted with the Nanoplotter 2.0, the surface was blocked with 2% BSA, and then incubated with 2 µg/ml streptavidin-Cy3 (Life Technologies, excitation at 550 nm, emission at 570 nm) to bind to antibodies and image their distribution and intensity.

Silver-enhanced bacteria were imaged under bright and dark field using a Nikon LV150A inspection microscope. Images were captured using a Nikon Digital Sight DS-Fi1 CMOS camera. Time course video of refractive index matching of PMMA microbeads with ammonium thiocyanate was captured with a Panasonic Lumix GH3 DSLR camera mounted to a Leica MZ8 stereomicroscope with a CMOS adapter.

Image analysis and particle counting of bacteria was conducted using ImageJ software (National Institutes of Health). Automatic particle counting in ImageJ was done by converting images to grayscale, and then to binary based on an intensity threshold. The “Watershed” algorithm was used to segment particles touching each other based on the estimated bacterium size, and the “AnalyzeParticles” plugin was used to estimate the number and size distribution of particles. Manual counting was done to verify the estimates of automatic particle counting.

3.0 Results and Discussion

A proof-of-concept assay for bacteria detection was demonstrated using the common lab strain *E. coli* K-12 and an attenuated strain of the pathogenic *E. coli*

O157:H7. Two types of binders for *E. coli* capture were investigated, bacteriophage (or phage) and antibodies. T4 phage capable of targeting the common lab strain *E. coli* K-12 were first tested as a potential binder for *E. coli* capture (Section 3.1). Next, antibodies were investigated as a binder for the capture and detection of *E. coli* O157:H7 (Section 3.2). Antibodies were found to capture bacteria with high density and low background, and were chosen as the binders to conduct a sandwich assay based on silver enhancement (Section 3.3). This was found to be an effective way to detect bacteria without the need for fluorescent microscopy. Next, a packed bed of microbeads was proposed to improve the assay sensitivity by increasing the surface area available for capture (Section 3.4). To eliminate imaging artifacts from the packed bed of microbeads, a refractive index matching method was developed, and used to image silver amplified bacteria on beads with improved sensitivity.

3.1 Bacteriophage Capture of *Escherichia coli* K-12

T4 phage were tested as a potential binder for capture of *E. coli* K-12 from solution. First, T4 were covalently linked to a glass slide, demonstrating capture versus non-specific binding on a blocked surface (Section 3.1.1). To reduce variability and demonstrate phage capture versus background, patterning techniques were explored. Phage were microcontact printed (Section 3.1.2) and spotted as is done with protein microarrays (Section 3.1.3).

3.1.1 Immobilization of T4 Bacteriophage

Capture of *E. coli* K-12 by immobilized T4 phage on glass was first demonstrated. A glass slide functionalized with APTES and activated with glutaraldehyde (Section 2.5) was separated into blocks using a 16-well gasket. Wells

were incubated with 100 μl of T4 phage (10^9 pfu/ml) for 3 h, followed by blocking with 2% BSA to prevent non-specific binding of *E. coli*. As a negative control, wells on the same slide were blocked with 2% BSA. *E. coli* K-12 culture (10^9 cfu/ml) was incubated on the slide for 30 min, followed by washing with PBS, and the slide was imaged by fluorescent microscopy. It was found that the T4 phage-coated surface captured *E. coli* K-12 from solution as expected (Fig. 4A), while the negative control showed significantly lower capture resulting from non-specific binding (Fig. 4B).

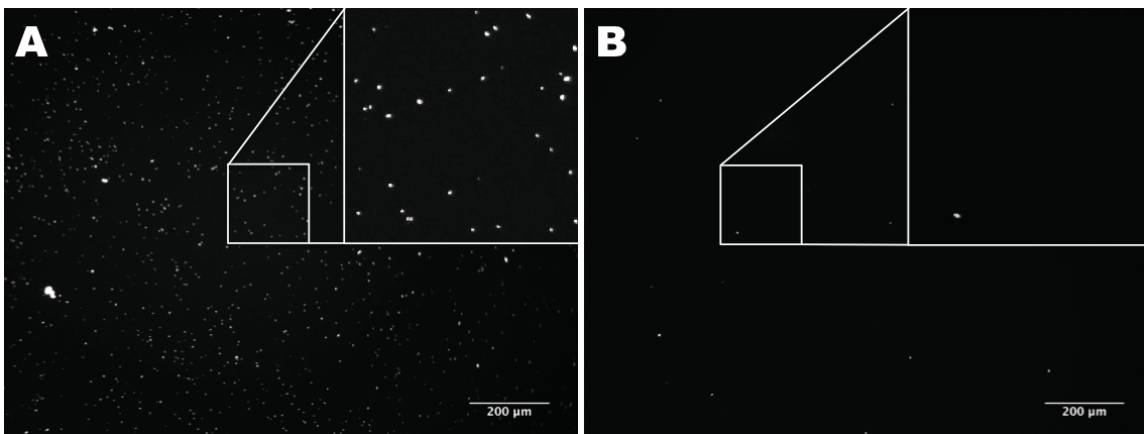


Figure 4: Fluorescent micrograph showing capture of *E. coli* K-12 by T4 bacteriophage on reactive aldehyde-coated glass. A) APTES/glutaraldehyde functionalized surface covalently bound to T4 bacteriophage captures *E. coli* K-12 compared with B) significantly lower capture on a negative control of APTES/glutaraldehyde-coated glass blocked with BSA.

While this approach was shown to be effective in capturing bacteria from the sample, it was also highly variable. Depending on where the slide was imaged, *E. coli* capture density varied significantly, making it challenging to attribute a capture density solely to phage. This was especially problematic near the edges of wells, where a high density of bacteria capture was often observed, likely resulting from variations in shear

stresses in the well at the corners and edges during washing (conducted using a shaker at 200 rpm) (Fig. 5A). Similarly, when a droplet of phage solution was incubated on the surface, a ‘coffee ring’ effect was frequently observed (Fig. 5B). This results from particles being concentrated at the droplet edge as drying occurs due to capillary effects (Deegan et al., 1997).

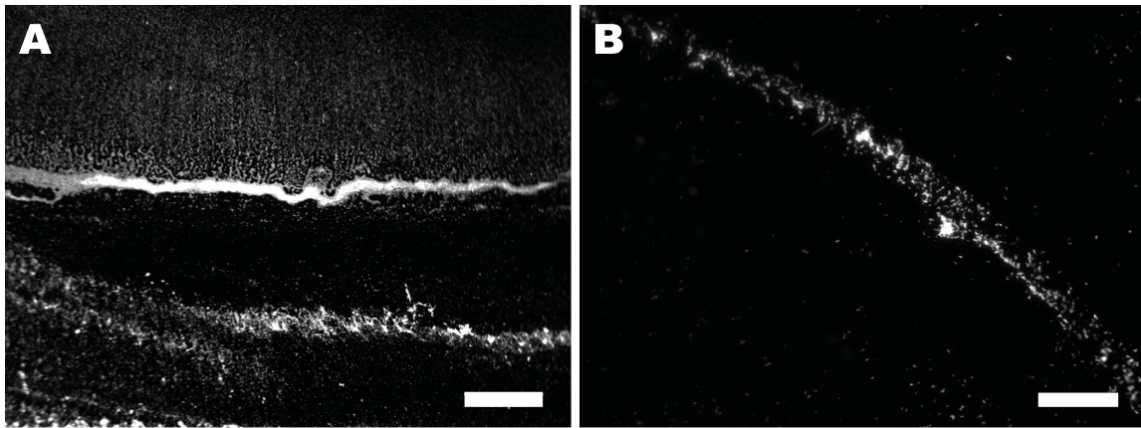


Figure 5: Variations in the capture of *E. coli* K-12 by T4 phage immobilized on reactive aldehyde-coated glass. A) High density of *E. coli* K-12 capture observed at the edge of wells. Scale bar shows 200 μm . B) Coffee ring effect of captured *E. coli* K-12 by T4 phage immobilized by a droplet incubated on the surface. Scale bar shows 100 μm .

Factors such as shear stress during washing and variations in density of functional groups for phage immobilization likely effect the capture of *E. coli* considerably. Thus, several methods to pattern T4 phage were explored in an attempt to reduce these variations at the ‘macroscale’, allowing the capture of *E. coli* by phage and the non-specific binding with negative controls to be compared locally at the microscale.

3.1.2 Microcontact Printing of T4 Bacteriophage

One such method investigated to pattern phage at the microscale was microcontact printing. In microcontact printing, a protein solution is incubated on a PDMS stamp, then gently rinsed, resulting in a monolayer of protein adsorbed to the surface. The stamp is then brought into contact with a substrate of higher surface energy, and the protein is transferred with high fidelity (Bernard, Renault, Michel, Bosshard, & Delamarche, 2000). This was attempted with T4 phage on various surfaces. First, an APTES/glutaraldehyde-activated surface was tested to covalently link phage to the surface. However, this was unsuccessful because proteins transferred by microcontact printing typically adhere to the surface through physisorption (Bernard et al., 2000). It is probable that the covalent linkage of phage to glutaraldehyde is more kinetically favorable in liquid solution, where the mobility can allow for binding. Rather than covalent linkage, physisorption of phage to PLL-coated glass was investigated. PLL has a net positive charge at neutral pH (Rainaldi, Calcabrini, & Santini, 1998) and *E. coli* phage, including T4, have an overall negative charge at neutral pH (Krueger, Ritter, & Smith, 1929). It was hypothesized that electrostatic interactions would immobilize phage to the PLL-coated surface through physisorption.

Stamps with 125 μm wide channels (separated by 125 μm) were used to microcontact print stripes of T4 phage on PLL. 10 μl of phage stock solution (10^9 cfu/ml) was deposited on the surface of stamps, and covered with a cover slip to evenly distribute the solution. After roughly 30 min of incubation under high humidity, stamps were gently rinsed with PBS and distilled water and dried under nitrogen. Stamps were brought into contact with a PLL surface for 30 s. After stamp removal, the surface was blocked with

2% BSA and rinsed with PBS. As a negative control, a blank stamp (incubated with PBS) was also printed to ensure the stamping process did not influence bacteria capture. The printed surfaces were incubated with *E. coli* K-12 (10^7 cfu/ml) for 30 min and imaged by fluorescence microscopy.

Stripes of captured *E. coli* K-12 equal to the width of channels on the PDMS stamp were observed (Fig. 6A), separated by stripes of low density, likely resulting from non-specific binding. The distribution of *E. coli* capture on stripes varied significantly (Fig. 6B), which could be attributed to the ineffective immobilization of phage. The capture density was not as high as anticipated and is likely limited, since only a monolayer of proteins (or in this case, phage) are transferred to the surface in microcontact printing. Therefore, the density of immobilized phage is limited by how tightly phage can pack on the surface of the PDMS stamp, and the efficiency of transfer. Moreover, the structure and directional binding abilities of phage (binding occurs via tail fibers only), suggests only a portion of transferred phage would immobilize in the proper orientation for bacteria capture. A characterization step, such as electron microscopy, could further elucidate the density and orientation of immobilized phage and should be examined in future work on approaches for microcontact printing phage. However, it was expected that alternative approaches using covalent linkage could increase the density and improve the patterning of phage for bacteria capture.

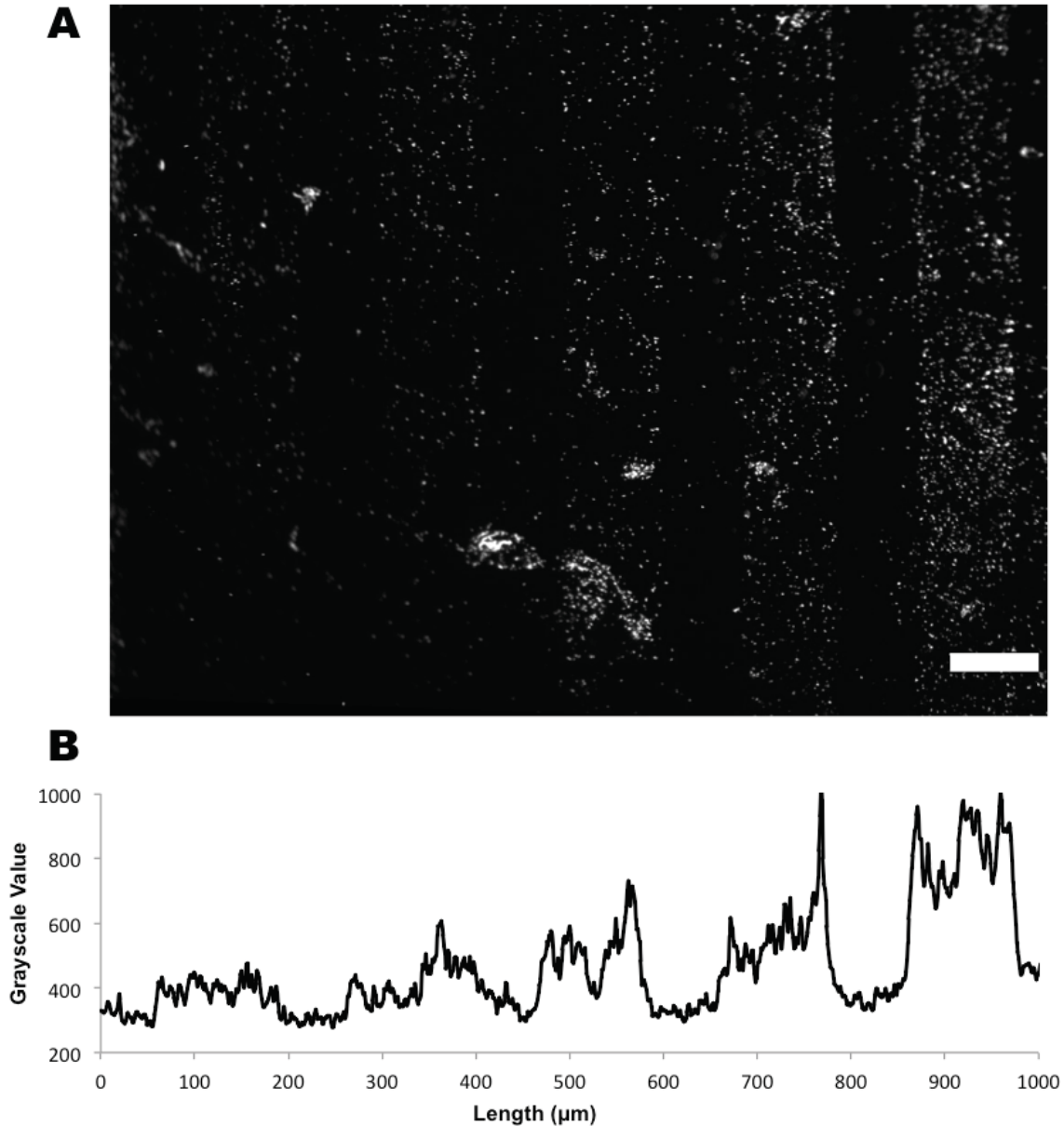


Figure 6: Microcontact printed T4 bacteriophage on poly-L-lysine-coated glass captures stripes of *E. coli* K-12. A) Fluorescent micrograph of GFP-expressing *E. coli* K-12 captured by microcontact printed T4 bacteriophage on PLL. Scale bar shows 100 μm . B) Grayscale intensity measurement showing stripes were printed, however the variation of captured *E. coli* varies significantly.

3.1.3 Microarray Printing of T4 Bacteriophage

To produce precisely defined patterns and increase the density of immobilized phage for bacteria capture, a microarray patterning technique was employed. Protein

microarrays consist of an array of different immobilized antibody spots for antigen detection, allowing for high-throughput experiments and multiplexed assays at the microscale (MacBeath, 2002). To optimize the printing of phage, the concentration, pH and printing buffer of phage solutions were varied, and different combinations were spotted onto surfaces such as APTES/glutaraldehyde-functionalized glass or Xenobind® to investigate covalent linkage, and PLL-coated glass to investigate physisorption. Following spotting, slides were left to react overnight, then blocked with BSA. Using a 16-well gasket to separate blocks printed under different conditions, each well was incubated with 200 μ l of *E. coli* K-12 culture (10^7 cfu/ml) for 30 min and imaged by fluorescent microscopy.

In initial experiments, the phage-binding capacity of surfaces was examined. Five rows of phage dilutions (each with 8 replicate spots) were spotted for each pH and printing buffer condition (microarray slide layout and printing buffer descriptions in Section 2.5). The first solution (1:0 ratio) contained undiluted phage (10^9 pfu/ml) in SMG buffer. Subsequent rows were diluted with printing buffers (1:1, 1:4, 1:8) at varied pH (7.5, 8.0, 8.5, 9.0). The final row (0:0) was printed with pure printing buffer (no phage) as a negative control (Table 1).

Table 1: Bacteriophage dilutions for microarray spotting experiments

<i>Ratio</i>	<i>Concentration</i>
1:0	1.0×10^9 pfu/ml
1:1	5.0×10^8 pfu/ml
1:4	2.0×10^8 pfu/ml
1:8	1.1×10^8 pfu/ml
0:0	negative control

Of the surfaces examined (APTES/glutaraldehyde, Xenobind®, PLL), the clearest results were observed on the reactive aldehyde-coated surface of Xenobind®. A decrease in the capture density of *E. coli* K-12 could be seen with the rows of phage dilutions (Fig. 7). It was found that high pH (9.0) in 50% glycerol printing buffer improved the immobilization of phage (as determined by the amount of *E. coli* capture). Pure phage in SMG (1:0) was not effectively immobilized, likely due to the neutral pH of the solution limiting the efficacy of covalent linkage. The area surrounding the printed spots, blocked with BSA, showed low capture of *E. coli* K-12, suggesting the blocking protocol was effective in preventing non-specific binding.

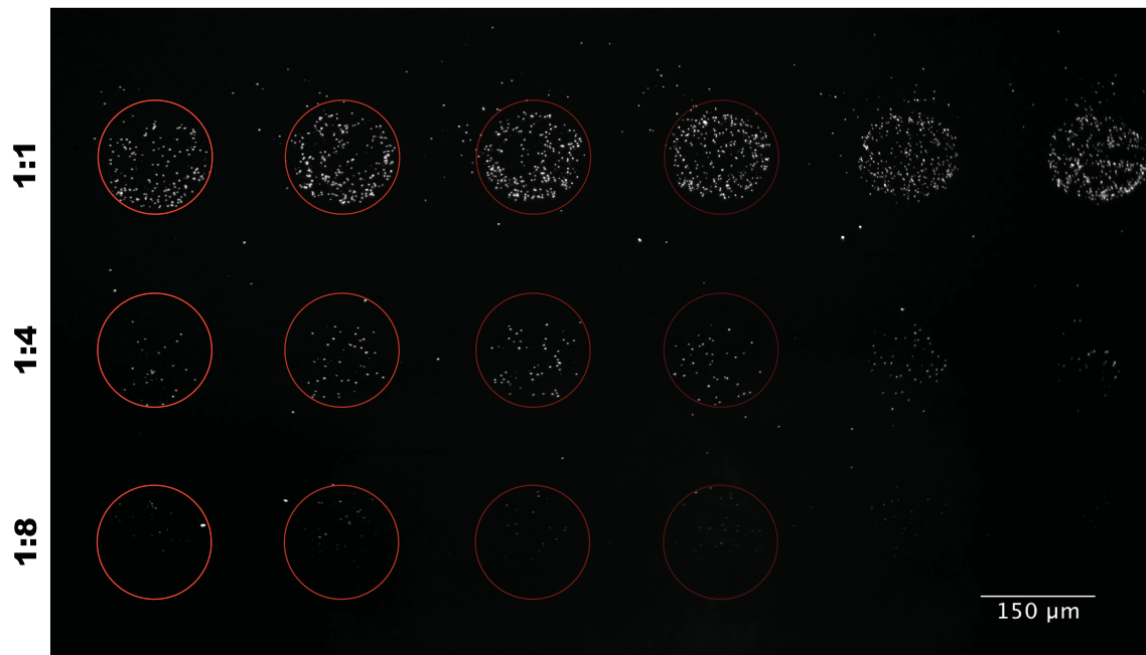


Figure 7: *E. coli* K-12 capture by microarray of T4 phage dilutions. Highest capture densities of *E. coli* K-12 observed at pH 9.0 printed in a 1:1 ratio (see Table 1) with 50% glycerol. Red circles of 150 μm diameter where spots were printed are added for visualization purposes. Phage dilution ratios listed on the left. Data for 1:0 and 0:0 not shown (no capture observed).

It was noted that the highest concentration of phage in printing buffer (1:1 ratio) resulted in the highest density capture of *E. coli*. Given the concentration of phage, combined with the small volume delivered by the microarray (assuming nanoliter volume and 10^9 pfu/ml, this equates to only ~ 1000 phage per $150\ \mu\text{m}$ diameter spot), it was presumed that a higher density of captured cells could be achieved with an increased phage titer. Efforts were made to increase the T4 phage titer to repeat microarray experiments with higher phage concentrations. Using a liquid phase propagation protocol (Section 2.2), a T4 phage titer of 10^{12} pfu/ml was obtained, and microarray experiments were repeated using a 1:1 ratio with printing buffers at varied pH. At high pH (9.0) in 50% glycerol printing buffer, a high density of captured *E. coli* was achieved on reactive aldehyde surfaces. Xenobind® had a high surface binding capacity and low background (Fig. 8A) when compared to APTES/glutaraldehyde, where visible streaking of immobilized phage could be observed (Fig. 8B).

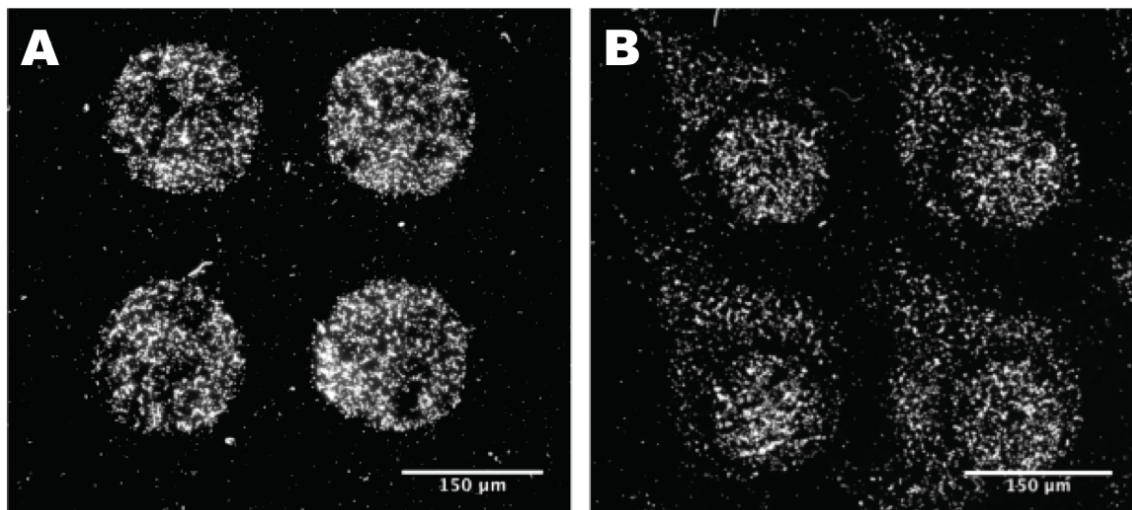


Figure 8: High titer of spotted T4 bacteriophage capture GFP labeled *E. coli* K-12 with high density on reactive aldehyde coated surfaces at pH 9.0. A) Xenobind® reactive aldehyde and B) APTES/Glutaraldehyde. Visible streaking of captured cells with the

APTES functionalized surface suggests the binding capacity of the surface was exceeded. Scale bar shows 150 μm .

The immobilization of phage on Xenobind was strongly affected by both printing buffer and pH. It was found that the 50% glycerol buffer produced a higher density of *E. coli* capture than 2M betaine/25% + 1,3-butanediol at equivalent pH (Fig. 9), presumably from an increased density of immobilized phage on the surface. It was determined that the optimal conditions for T4 phage immobilization were at high pH (9.0) in 50% glycerol on Xenobind® glass, yielding an *E. coli* capture density of roughly 2.5×10^4 *E. coli*/mm². Blocking with 2% BSA was shown to sufficiently reduce non-specific binding, allowing capture to be attributed to the patterned phage.

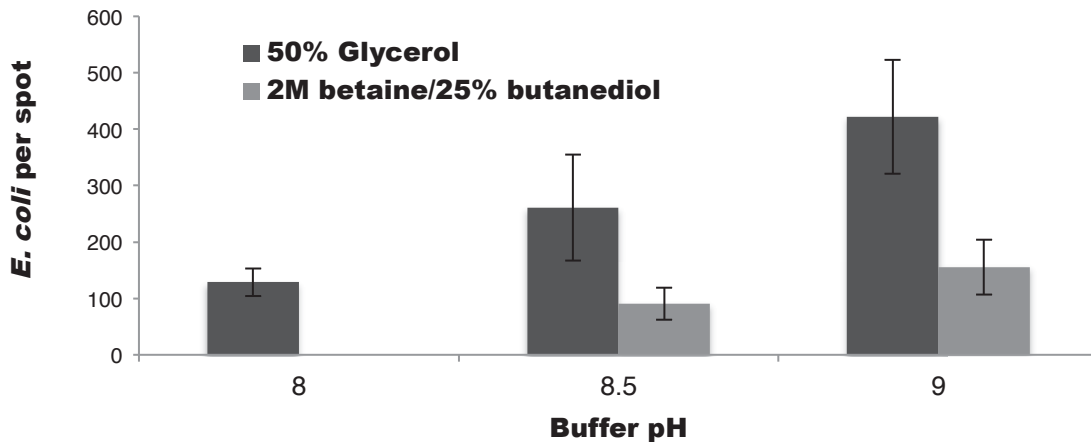


Figure 9: Effect of printing buffer and pH on the density of captured *E. coli* by immobilized T4 phage on Xenobind®. 50% glycerol improves the immobilization of T4 phage when compared to 2M betaine/25% 1,2-butanediol at equivalent pH. T4 phage immobilization is improved with pH up to 9.0. Spot diameter was 150 μm . Results for pH 7.5 not shown due to insufficient *E. coli* capture.

Here, T4 phage were shown to effectively capture *E. coli* K-12 from solution with high surface density. However, one drawback to using phage as a capture binder for

bacteria detection is that the viruses often lyse captured cells within an hour or two, making it difficult to complete subsequent detection steps of the assay. It is possible that this time constraint due to cell lysis could be reduced or eliminated by using non-lytic (i.e. lysogenic) phage, or by using ‘ghost phage’ that have the nucleic acids removed to prevent virion replication (Duckworth, 1970).

It was observed that *E. coli* captured by phage were sensitive to shear stress during washing steps, influencing the capture density significantly. A trade off between sufficient washing to eliminate background capture and limiting shear stress to maintain a high density of *E. coli* capture was evident. This might be attributed to the binding affinity of T4 phage to the captured bacteria, or the number of phage that bind to each cell. It is expected that the bacteria will experience shear forces during washing steps that could potentially detach them the phage binders. Alternatively, it is known that the long tail fibers of the phage can be detached from the capsid with sufficient shear force (Esposito et al., 1996), and it is possible that during washing the long tail fibers could be broken. The shear stress sensitivity of bacteria captured by phage should be examined further in future work. However, it is clear that phage offer one approach for the capture of bacteria samples from solution with good efficiency.

3.2 Antibody Capture of *Escherichia coli* O157:H7

Alternative approaches to phage for the capture and detection of *E. coli* were explored with the use of antibodies. The use of antibodies for the capture and detection of antigens is currently more established than biosensors which utilize phage. Antibodies tagged with markers or moieties for subsequent detection steps are often available from suppliers, reducing the time, effort and cost that would be required to tag phage for

subsequent detection steps. If antibodies for a given pathogen are not already available, they can often be produced through immunization of an animal host with the antigen, however this can be laborious. While the production of phage is cheaper and arguably more humane than the production of antibodies, phage are generally isolated from naturally occurring samples containing high bacteria diversity (e.g. sewage water) and screened for selectivity. If the phage is lytic, the destruction of the host cell may also be detrimental to detection by immunoassay, however this can be avoided with the use of ‘ghost phage’ which have their genetic material removed to prevent virion replication. For these reasons, antibodies were selected as an alternative to phage for the capture and detection of bacteria. To demonstrate the ability of antibodies to efficiently capture pathogenic strains, an attenuated strain of *E. coli* O157:H7 was used with anti-O157:H7 for capture and anti-*E. coli* O & K for detection (Section 2.3).

3.2.1 Optimization of Antibody Immobilization

The immobilization of antibodies was optimized using the microarray platform following similar conditions for phage printing. A range of pH values (7.5, 8.0, 8.5, 9.0) was tested using antibodies suspended in 50% glycerol or 2M betaine/1,3-butanediol printing buffers. Surfaces for covalent binding were tested using Xenobind®, APTES/glutaraldehyde and Epoxy slides (Table 2).

Table 2: Summary of microarray substrates

Substrate	Supplier	Chemistry
Nexterion®	Schott	Reactive epoxide
Xenobind®	Xenopore	Reactive aldehyde
APTES/Glutaraldehyde	-	Reactive aldehyde

Biotinylated antibody dilutions against O and K serotype *E. coli* were printed, then incubated with 2 µg/ml streptavidin-Cy3 for fluorescence imaging using an Agilent scanner (Section 2.8). Antibody dilution ratios used to test binding capacity can be found in Table 3.

Table 3: Antibody dilutions for microarray printing experiments

Row	Ratio	Concentration
1	1:1	200 µg/ml
2	1:3	66.6 µg/ml
3	1:9	22.2 µg/ml
4	1:27	7.40 µg/ml
5	1:81	2.47 µg/ml
6	1:243	0.823 µg/ml
7	1:729	0.274 µg/ml
8	1:2187	0.0914 µg/ml
9	0	Negative Control

It was found that all surfaces were able to covalently link antibodies, and 2% BSA was sufficient in blocking the surface. Unlike the printing of phage on the microarray platform, 2M betaine with 25% 1,3-butanediol was found to be more effective in immobilizing antibodies (Fig. 10, right), as seen by the improved capture at higher antibody dilutions. It is possible that glycerol inhibits the binding of antibodies on these surfaces via its increased viscosity, whereas for phage, increased viscosity may have better preserved the structure. Epoxy surfaces had the lowest binding capacity, as observed by the inability to immobilize antibodies in the printed regions (Fig. 10, top row). It also appears that printing solutions were not effectively transferred to the surface, as seen by the rectangular shape of immobilized antibodies where the pin directly contacted the surface. Both Xenobind® (Fig. 10, middle row) and APTES/glutaraldehyde (Fig. 10, bottom row) showed improved spot morphology and good binding capacity.

While at the highest concentrations of antibody (200 $\mu\text{g}/\text{ml}$, top row), it appears the Xenobind® surface binding capacity was exceeded, the spot diameter in every row is also smaller than for APTES/glutaraldehyde, where the solutions appear to spread out. This suggests that the Xenobind® surface concentrates antibodies more densely, however both reactive aldehyde surfaces appear sufficient for antibody immobilization. Xenobind® was therefore chosen to demonstrate antibody capture of *E. coli* O157:H7.

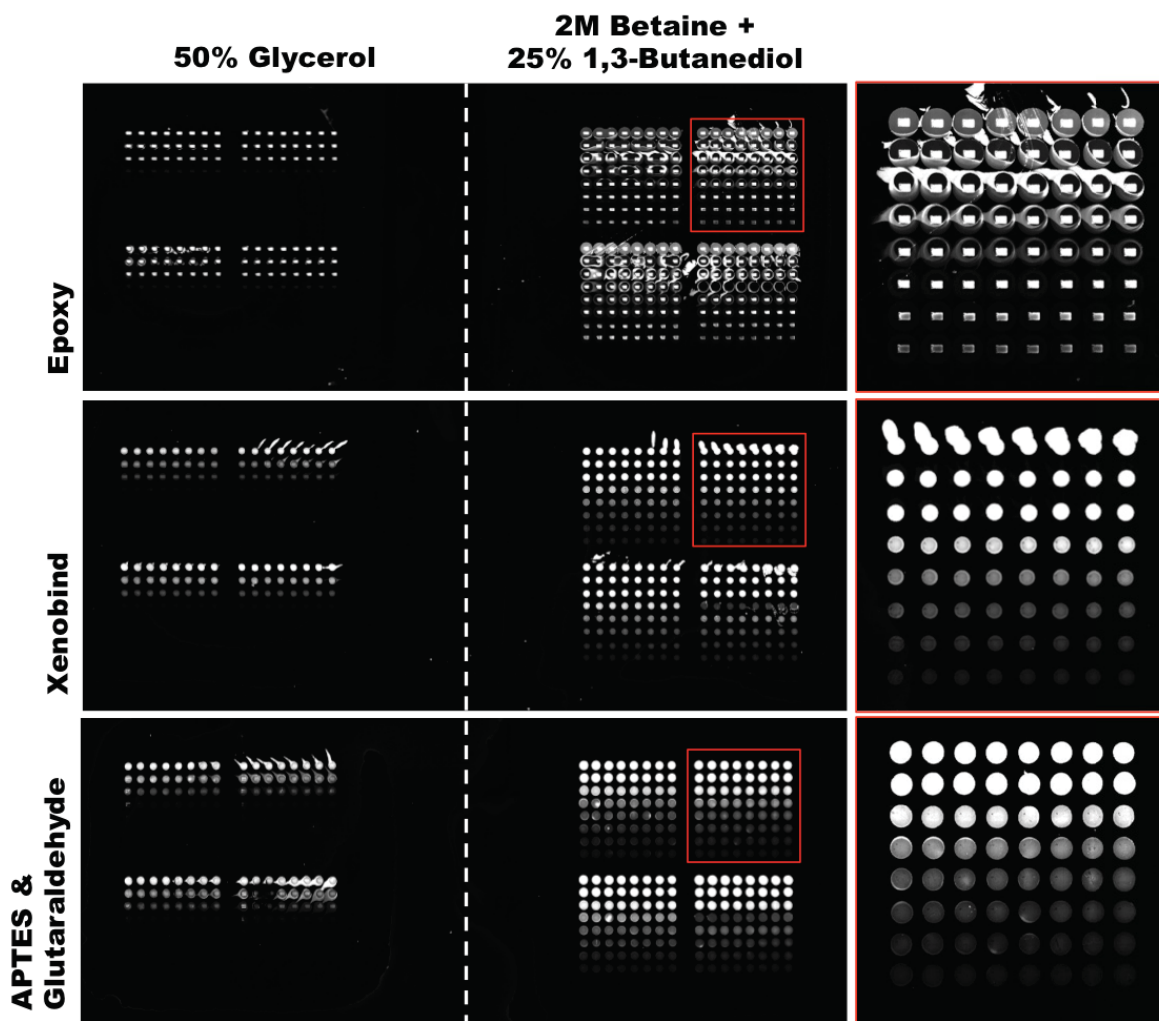


Figure 10: Optimization of antibody printing conditions. Three surfaces were examined for antibody immobilization: Epoxy, Xenobind® and APTES/Glutaraldehyde. Hygroscopic printing buffers used were 50% glycerol (left) and 2M betaine with 25%

1,3-butanediol (right) using buffer pH values 7.5, 8.0, 8.5, 9.0. Optimal conditions found at blocks of pH 9.0 (shown here).

3.2.2 *Escherichia coli* Capture by Antibodies

Antibody capture of *E. coli* O157:H7 was also demonstrated using the microarray platform and compared with the non-specific binding of the background (blocked with 2% BSA) to ensure the chosen antibodies were able to reliably capture cells in high density. Based on antibody immobilization results (Section 3.2.1), antibodies were printed on Xenobind® glass at a concentration of 100 µg/ml, followed by blocking for 2 h with 2% BSA. Slides were incubated with *E. coli* O157:H7 (10^7 cfu/ml) stained with SYTO® 9 for 30 min, followed by washing with PBS for 5 min at 200 rpm on the ThermoShaker (×3), then imaged by fluorescent microscopy.

It was found that anti-*E. coli* antibodies, against O and K serotypes, captured *E. coli* O157:H7 with high density and comparably low background (Fig. 11). As a negative control, anti-*E. coli* spots were incubated with *E. coli* K-12 under the same conditions, however, no capture was observed since the K-12 strain does not possess O or K surface antigens. It was noted that *E. coli* captured by antibody spots were considerably less susceptible to shear stress during washing steps, suggesting that antibodies are capable of binding more strongly to captured cells than phage. Additionally, cells captured by antibodies did not face the same challenges with lysing as those captured by phage.

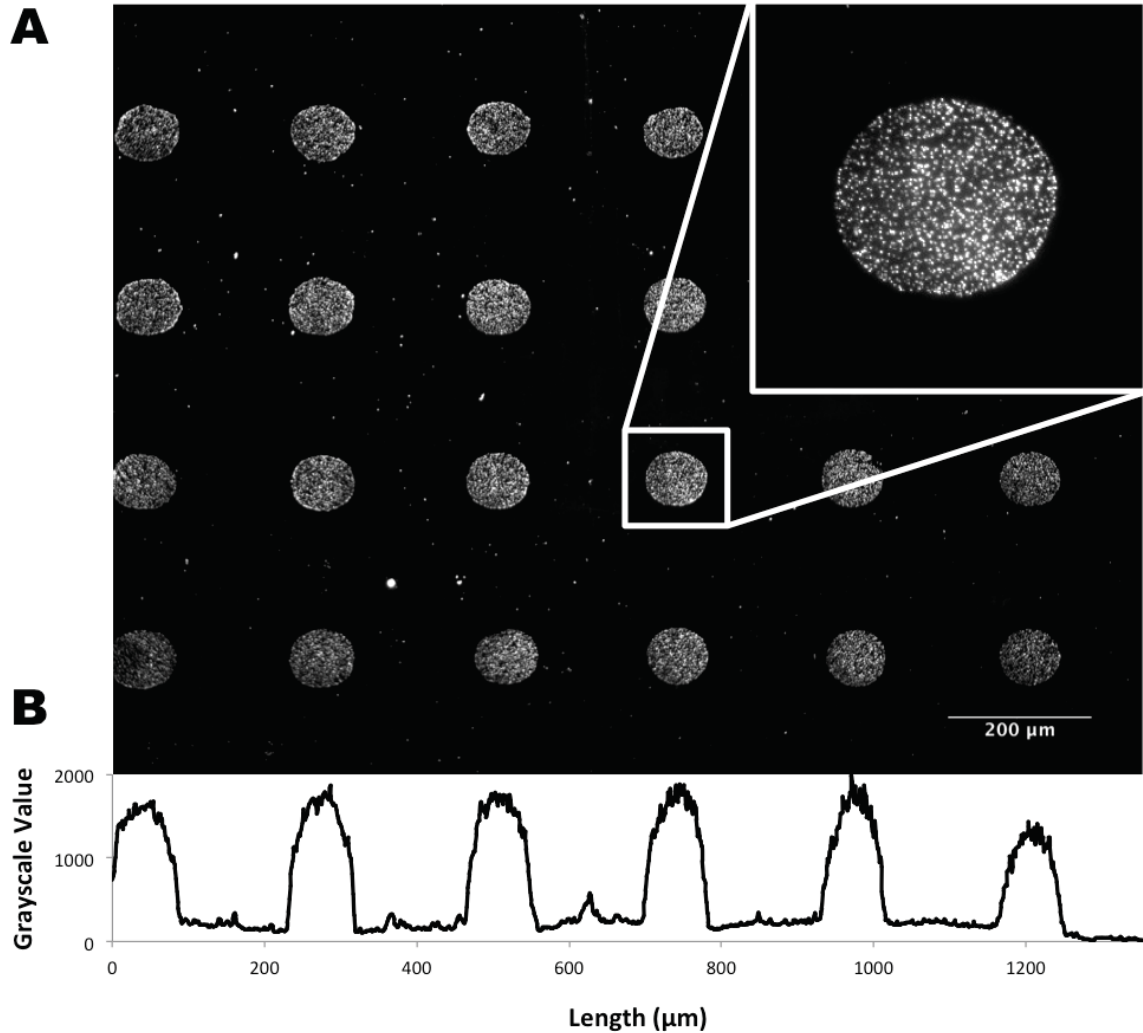


Figure 11: Spotted antibodies capture *E. coli* O157:H7 with high density and low background. A) Florescent micrograph of *E. coli* O157:H7 captured by spotted anti-*E. coli* printed at 100 $\mu\text{g}/\text{ml}$ followed by blocking with BSA. Scale bar shows 200 μm . Inset shows magnified view of a single spot with captured *E. coli* O157:H7. B) Grayscale intensity plot of array showing uniform capture of *E. coli* cells in spots and comparably low background.

Experiments were repeated with spots of anti-*E. coli* O157:H7 antibody. While this antibody was also able to capture *E. coli* O157:H7, strange patterns of captured cells were observed that were repeatable (Fig. 12). Similar patterns were observed using either 50% glycerol or 2M betaine, 1,3-butanediol over a range of pH values.

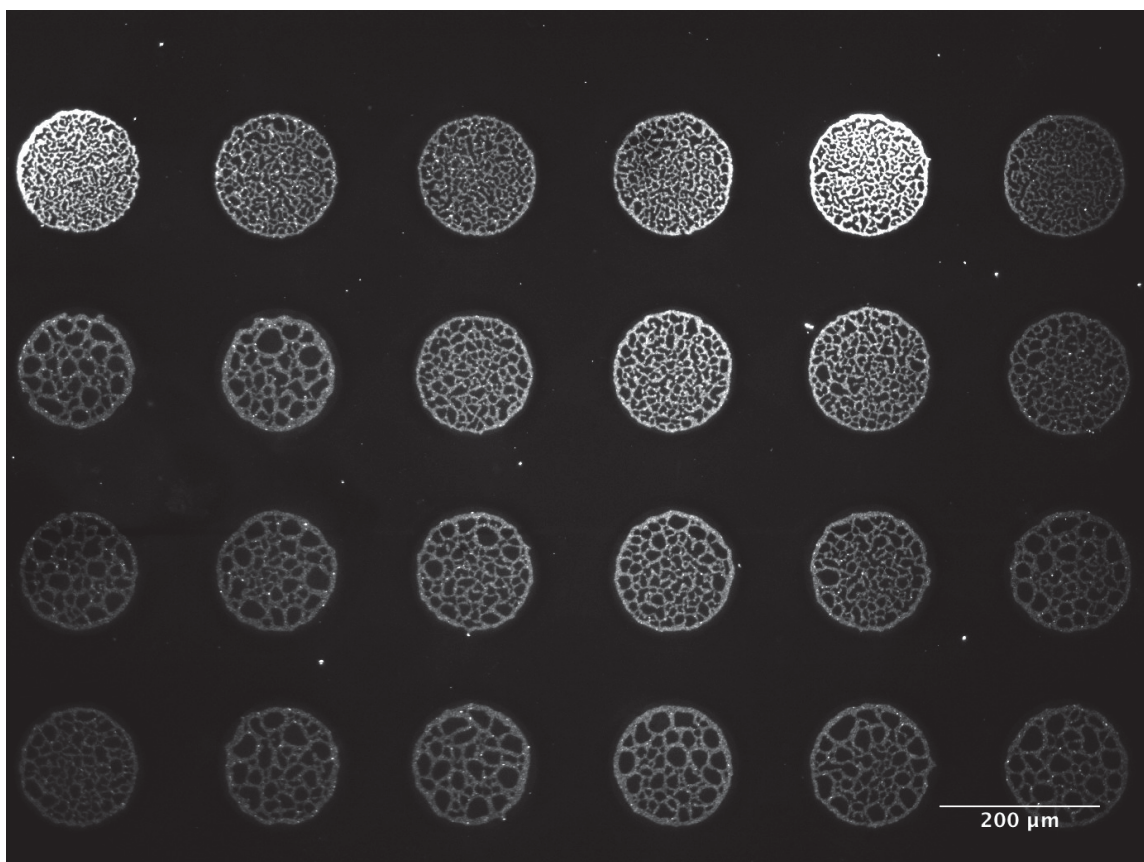


Figure 12: Fluorescent image of *E. coli* O157:H7 patterns captured by anti-O157:H7 antibodies. A microarray of anti-O157:H7 antibodies were printed with 2M betaine and 25% 1,3-butanediol at 100 $\mu\text{g}/\text{ml}$ on Xenobind® at pH 9.0, followed by incubation with SYTO® 9 stained *E. coli* O157:H7. *E. Coli* were captured in non-homogenous patterns, suggesting a problem with the antibody immobilization.

To verify that these patterns were a result of antibody immobilization, and not an artifact of downstream steps, anti-O157:H7 was reprinted and spiked with Alexa Fluor 405 (4 $\mu\text{g}/\text{ml}$) to visualize protein patterns (Fig. 13). It was observed that the *E. coli* (Fig. 13A) was captured in the same regions as proteins were immobilized (Fig. 13B), suggesting the antibody immobilization technique was responsible for generating these patterns.

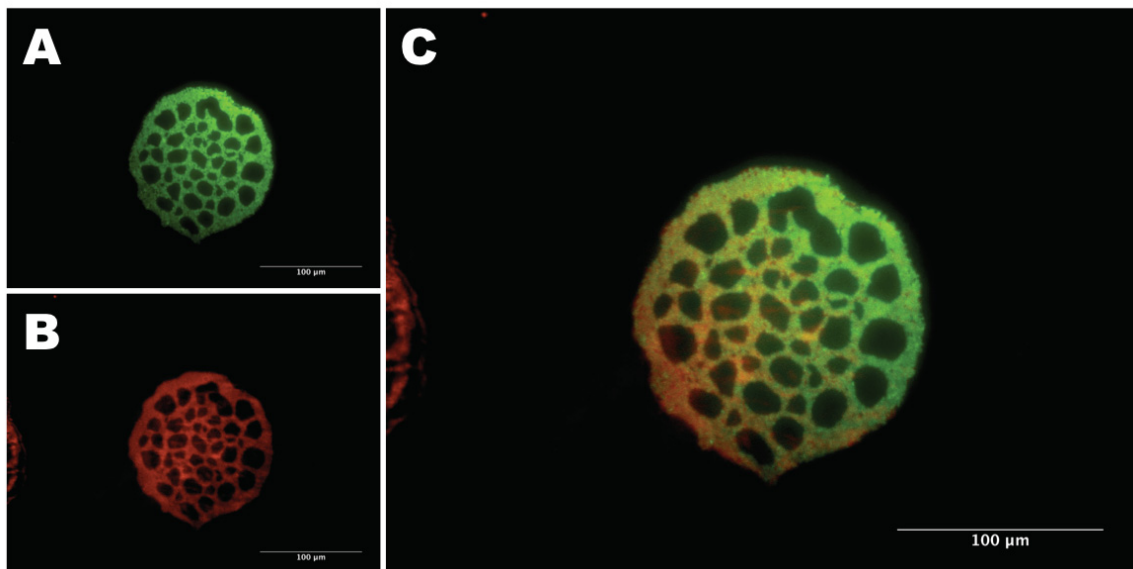


Figure 13: Fluorescent image showing patterns of captured *E. coli* O157:H7 results from irregularities in antibody immobilization. A) *E. coli* O157:H7 stained with SYTO® 9 are captured in the same regions as B) the immobilized antibodies (spiked with Alexa Fluor® 405) printed with 2M betaine +25% 1,3-butanediol (pH 9.0) on Xenobind® C) Merged image of *E. coli* O157:H7 and antibody distribution. Scale bars show 100 μm.

While the reason for these patterns is not understood, it is suspected that glycerol present in the storage buffer may have had a destabilizing effect on the protein, leading to inhomogeneity. It is well known that the addition of glycerol can lead to changes in the structure and dynamics of proteins from their native state (Scharnagl, Reif, & Friedrich, 2005). Another possibility is that protein stability, in terms of pKa, was disrupted under the basic conditions needed for covalent binding. However, despite these challenges with patterning, it was clear the antibody was effective in capturing *E. coli* O157:H7 with considerably low background. To avoid the formation of these patterns, flat glass surfaces were separated into blocks using 16-well gaskets, and a 200 μl volume of anti-O157:H7 antibodies were incubated in each well using a shaker to evenly distribute antibodies

across the surface. This provided more even distribution of antibodies on the surface than using the spotting technique.

Thus, it was demonstrated that both antibodies chosen were able to efficiently capture *E. coli* O157:H7 from solution easily within a 30 min incubation time. Blocking with BSA was highly effective in eliminating non-specific binding in the background. Antibodies were found advantageous over phage, given their lower sensitivity to shear stress and the elimination of problems posed by the lytic cycle. Antibodies were therefore used for capture and detection of *E. coli* O157:H7 in demonstrating a proof-of-concept assay for rapid pathogen detection.

3.3 Silver Enhancement for *Escherichia coli* Detection

Following demonstration of antibodies as an effective method to capture whole cells of *E. coli* O157:H7, a silver enhancement sandwich assay was developed. The purpose of the assay is to coat captured cells in a layer of reduced silver with the use of silver enhancement reagents. This should theoretically allow for detection without the need for fluorescence or high magnification microscopes, while still providing specificity for a target pathogen. Given a high enough concentration of cells, a net grayscale intensity of coated cells could be used to estimate concentration. At a threshold concentration, detection of low cell counts could be estimated by counting the number of dark, silver coated particles, offering potential for high sensitivity.

Here, an assay based on silver enhancement for detection of *E. coli* O157:H7 is proposed. Immobilized anti-O157:H7 antibodies are used for capture of *E. coli* O157:H7 from the sample solution, providing specificity and concentrating the target pathogen. Next, biotinylated anti-*E. coli* detection antibodies against O and K surface antigens are

incubated with the sample, coating the outer surface of the cells. Streptavidin-nanogold is introduced, and binds to detection antibodies providing a catalytic site on the bacteria surface for silver reduction. Finally, the sample is exposed to silver enhancement reagents, and a layer of silver is locally reduced on the cell surface (Fig. 14). Following this silver enhancement sandwich assay, captured *E. coli* O157:H7 become easily detectable as dark particles under bright field microscopy, or as reflective particles under dark field microscopy. This allows individual cells to be counted, offering potential for high sensitivity without the need for expensive fluorescent microscopes.

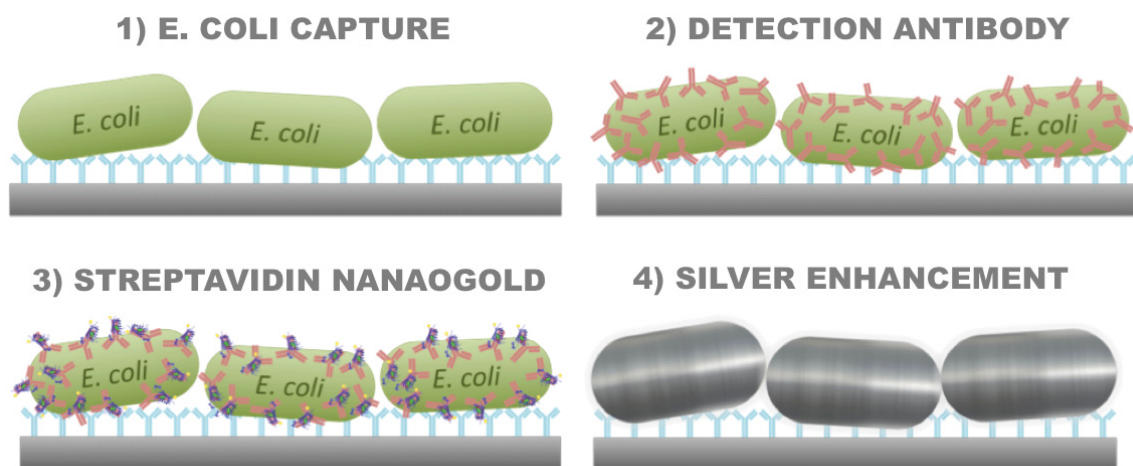


Figure 14: Schematic of a sandwich assay for the detection of bacteria by silver amplification. 1) *E. coli* is captured from the sample by immobilized capture antibodies specific against the target pathogen. 2) Captured cells are coated with a biotinylated detection antibody. 3) Streptavidin nanogold binds to the detection antibody. 4) Nanogold catalyzes the local reduction of silver.

The silver enhancement assay was performed on Xenobind® glass slides sectioned into blocks using a 16-well gasket. Half of the blocks were incubated with anti-O157:H7 antibodies (50 µg/ml) for 2 h while gently shaking (100 rpm) to uniformly distribute antibodies. The second half of the wells were blocked with 2% BSA to serve as

a negative control. Wells were then incubated with *E. coli* O157:H7 culture for 30 min, followed by biotinylated detection antibodies (20 µg/ml) for 30 min. Next, streptavidin-nanogold was incubated for 30 min, followed by washing with DI water before developing with silver enhancement reagents for 5 min, and thoroughly rinsing with DI water following development (Section 2.6).

Slides were imaged using dark field microscopy and captured *E. coli* were easily visualized as bright, reflective particles bound to the surface (Fig. 15A), compared to a negative control where little to no capture was observed (Fig. 15B). Even at low magnifications (i.e. 20x, Fig. 15C), silver-enhanced cells can be easily identified for counting. This suggests that in addition to eliminating the need for fluorescent microscopy, inexpensive imaging setups could potentially be used. This would decrease the cost of using such an approach for pathogenic bacteria detection, as inexpensive imaging equipment, such as USB microscopes which offer similar magnification ranges at low cost, could be used. It is presumed that at high enough concentrations of bacteria, the net grayscale value resulting from silver coated cells could be used to estimate cfu/ml, providing a very simple and low-cost reading. At low concentrations of cells, it is possible that detection could switch to a particle counting approach, where discrete silver coated bacteria are counted. Counting of individual cells could also be automated with particle counting software, providing a simple and quick readout of pathogen detection and concentration quickly and at low-cost. The steps of the assay, including washing between reagents, can be completed in under 2 h. By directly linking detection antibodies to nanogold, and optimizing the protocol, this could be reduced even further. Therefore,

the proposed detection scheme provides fast detection of pathogenic bacteria, and has potential to be a low-cost alternative to current detection mechanisms.

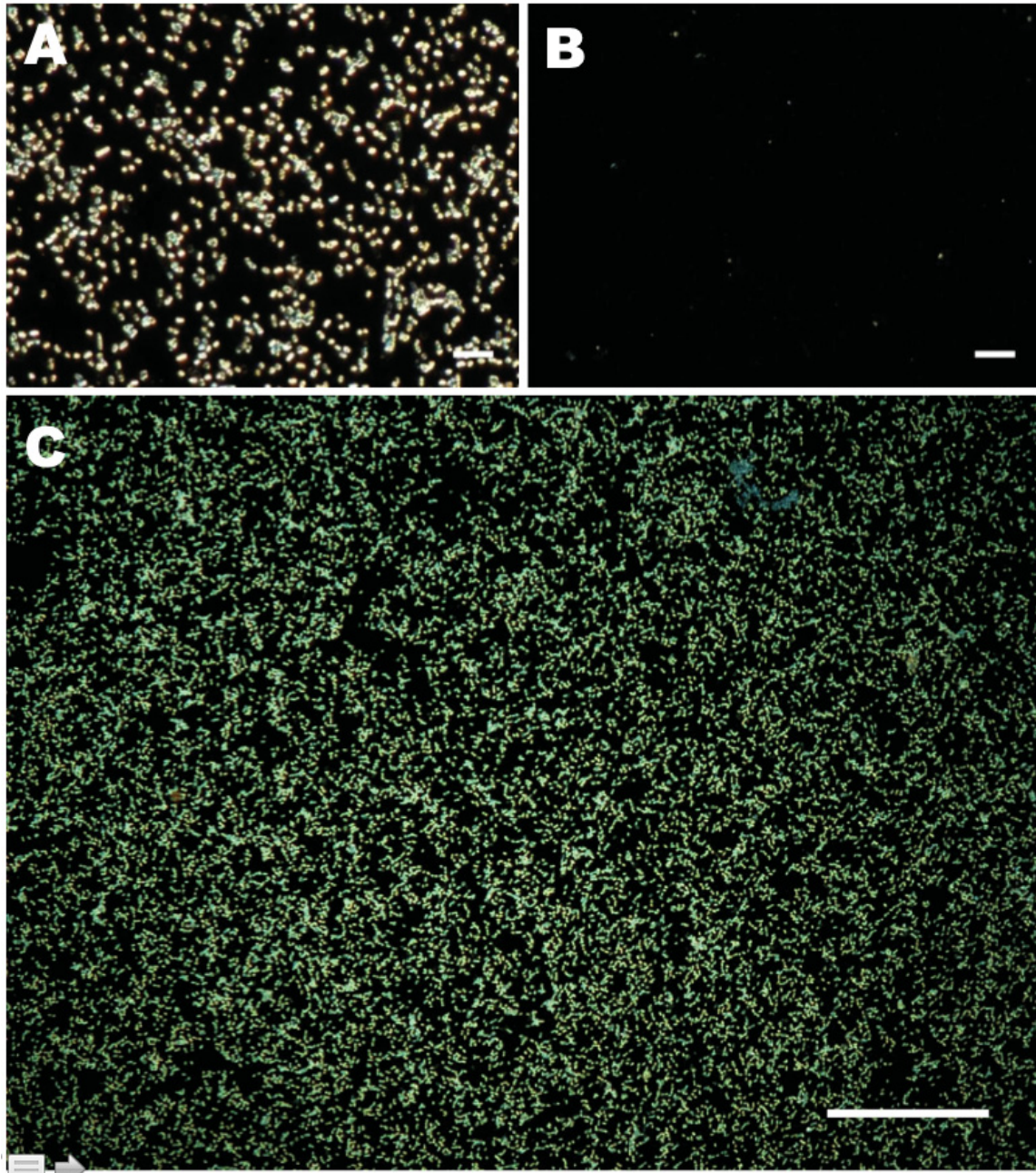


Figure 15: Dark field micrograph of silver enhanced *E. coli* O157:H7. A) Silver enhanced *E. coli* O157:H7 captured by anti-O157:H7 antibody and B) negative control blocked with 2% BSA where no capture is observed. Scale bars show 10 μm . C) low magnification (20x objective) view showing that individual cells are distinguishable. Scale bar shows 50 μm .

It was noted that developing the silver enhancement reagents for more than 5 min increased the background of the negative control. However, these background silver precipitates were smaller in size than the silver-coated *E. coli*, and could be distinguished as noise. Standard protocol suggests DI water be used for washing before and after silver enhancement, however this produces a hypotonic environment due to lack of solutes, and can result in the bursting of cells. This was observed in the silver-enhanced *E. coli* (Fig. 15A), which appeared to have lost some of their characteristic morphology.

Several alternative solutions for washing the chip while minimizing cell bursting before and after silver enhancement (25% glycerol, 50% glycerol, carbonate buffer, HEPES buffer, LB broth, PBS, Tris buffer) were tested. It was found that most of these solutions drastically increased both the background of the negative controls *and* the background of the captured bacteria, making cells indistinguishable. Carbonate buffer (~pH 9.0) was found to better preserve the morphology of captured cells than DI water (. 16A, 16B). However, this unfortunately also increased the background noise in negative controls from the spontaneous formation of silver precipitates (Fig 16C, 16D). This increased background noise can likely be attributed to an increased pH promoting the reduction of silver nitrate by hydroquinone.

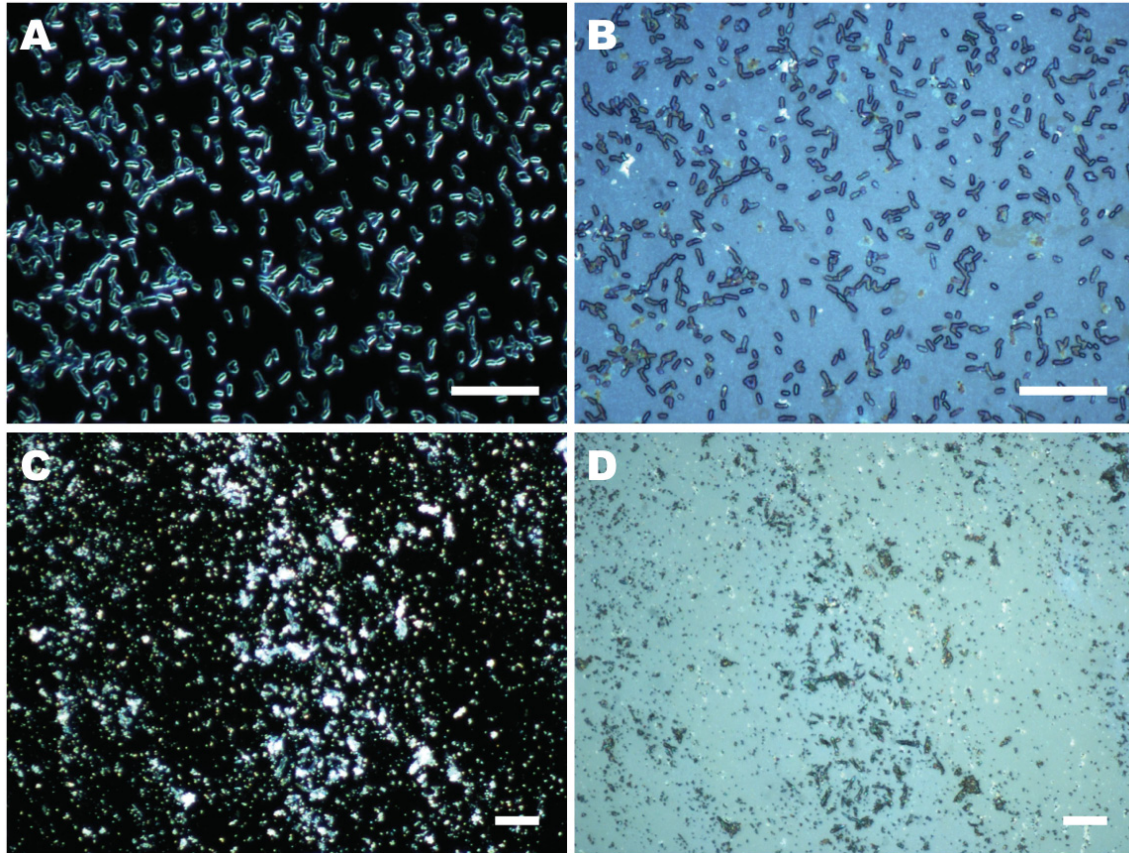


Figure 16: Carbonate buffer preserves the morphology of *E. coli* O157:H7 but increases background noise. A) dark and B) bright field micrographs of silver enhanced *E. coli* O157:H7 using carbonate buffer for washing. C) dark and D) bright field micrographs of negative controls show carbonate buffer also increases background noise by encouraging the spontaneous formation of silver precipitates. Scale bars show 10 μm .

Since DI water provided the lowest background, and cell morphology was still sufficiently preserved to identify and count captured *E. coli*, this was used as a wash buffer before and after silver enhancement. Future work might examine other buffers that maintain tonicity to better preserve cell morphology while preventing the formation of silver precipitates in negative controls.

A standard curve to estimate the sensitivity of the silver enhancement assay was performed. 10-fold serial dilutions of *E. coli* were incubated in the wells of immobilized

antibody and the wells of blocked surface (negative control for each dilution) for 30 min. Following completion of the assay, the number of silver enhanced bacteria were estimated in ImageJ. Briefly, a bright field image was converted to grayscale and thresholded to identify captured cells (Fig. 17). This was converted to binary, and the “Watershed” algorithm was used to separate touching cells (Fig. 17C, inset). The “AnalyzeParticles” plugin was then used to estimate the number and size distribution of particles, and was found to match with estimates from manual counting.

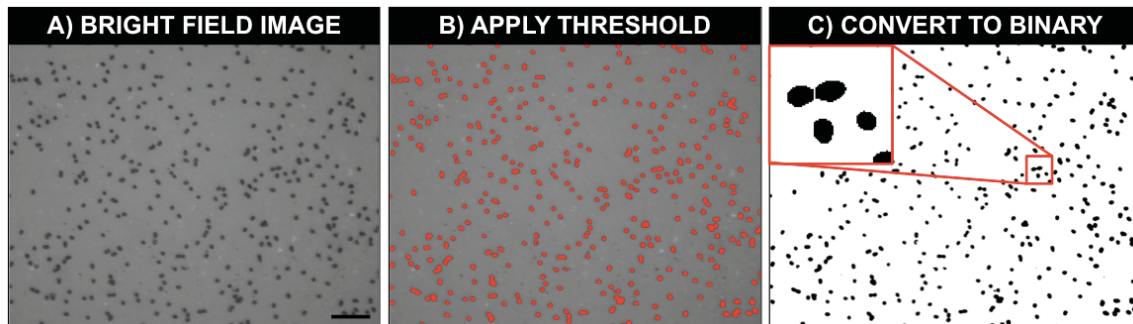


Figure 17: Particle counting approach in ImageJ for estimating capture density of *E. coli*. A) A bright field image is converted to grayscale and B) thresholded to identify cells. C) the image is converted to binary, and using the “Watershed” algorithm, touching particles are separated by a thin white line (inset). Scale bar shows 10 μm .

A standard curve based on the capture densities (*E. coli*/mm²) of performing the assay on a Xenobind® slide was produced (Fig. 18). A sensitivity of roughly 10⁷ cfu/ml was estimated. This sensitivity is low, and likely resulted from multiple wash steps between using each reagent, which were done using a ThermoShaker at 200 rpm in order to minimize background. However, the use of flat glass for conducting the assay is also inherently limited by the time required for diffusion or settling of bacteria to the surface for binding, but more importantly, the amount of surface area available for capture.

Therefore, methods to increase the interaction of bacteria with the surface, and increase the surface area available for capture, were investigated.

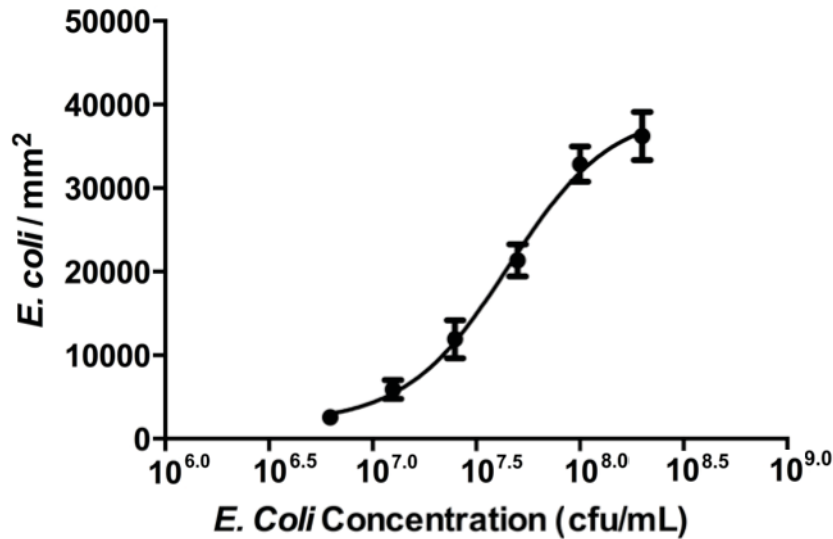


Figure 18: Standard curve for detection of E. coli O157:H7 on Xenobind® glass using the silver enhancement assay. A sensitivity of roughly 10⁷ cfu/ml was achieved, likely due to multiple washing steps and shear stress during the course of the assay, and the limited surface area available for capture.

3.4 Microbead Trap for Bacteria Capture

Efforts were made to improve the sensitivity of the assay by increasing the surface area available for capture using a packed bed of microbeads. Microbeads provide a high surface area (SA) to volume (V) ratio compared to flat surfaces; as the radius (r) of a microsphere decreases, the surface area increases by $3/\text{radius}$ (Eqn. 1). At the microscale, this increase becomes very significant, allowing for a high amount of surface area in considerably small volume.

$$\frac{SA}{V} = \frac{4\pi r^2}{\frac{4}{3}\pi r^3} = \frac{3}{r} \quad (\text{Equation 1})$$

Microbead diameters were chosen to allow sufficient space between beads for bacteria to pass (to reduce physical trapping) while being small enough to increase interactions of bacteria with the surface to enhance capture. The pores or spacing between microbeads is roughly 15% of the microbead diameter in a tightly packed-bed of spherical particles (Zeng & Harrison, 2007). Therefore, the microbeads selected (38-45 μm diameter) have pores on the order of 5.7-6.7 μm , sufficiently large to let bacteria 1-2 μm pass.

3.4.1 Microfluidic Bead Trap Design

A microfluidic bead trap with sieves of channels slightly smaller than the diameter of microbeads was designed, replicated in PDMS and used to produce the packed bed of microbeads (Section 2.7). Efficient and reproducible packing was first optimized to allow microbeads to be pre-immobilized with antibodies to be used directly to pack the chambers. The first iteration of the bead trap consisted of $1 \times 2 \text{ mm}^2$ and $2 \times 4 \text{ mm}^2$ chambers with 40 μm sieve channels (separated by 40 μm), 100 μm inlet and outlet channels and 1 mm diameter inlet and outlets (Fig. 19A). Two chambers were made on the same device; one for anti-O157:H7 coated beads, and a second for a negative control with BSA blocked PMMA beads to be run under the same conditions simultaneously. A 1 ml volume of bead suspension ($\sim 1\%$ w/v) was pumped into the inlet channels by hand. While bead packing was achievable with this design, it was not reproducible as beads often clogged at the inlets (Fig. 19A inset). The problem could not be fixed by reducing the bead concentration (to less than 0.01%), so a second iteration of the bead trap design

was produced. The improved design consisted of the same bead chamber dimensions, but with 300 μm inlet channels, 200 μm outlet channels, and curved inlets to guide the beads into the chamber and prevent clogging (Fig. 19B). This design allowed for reproducible and easy bead packing at concentrations of 1% w/v. Slightly smaller sieves (37 μm) were effective in trapping PMMA beads 38-45 μm in diameter (Fig. 19B, inset).

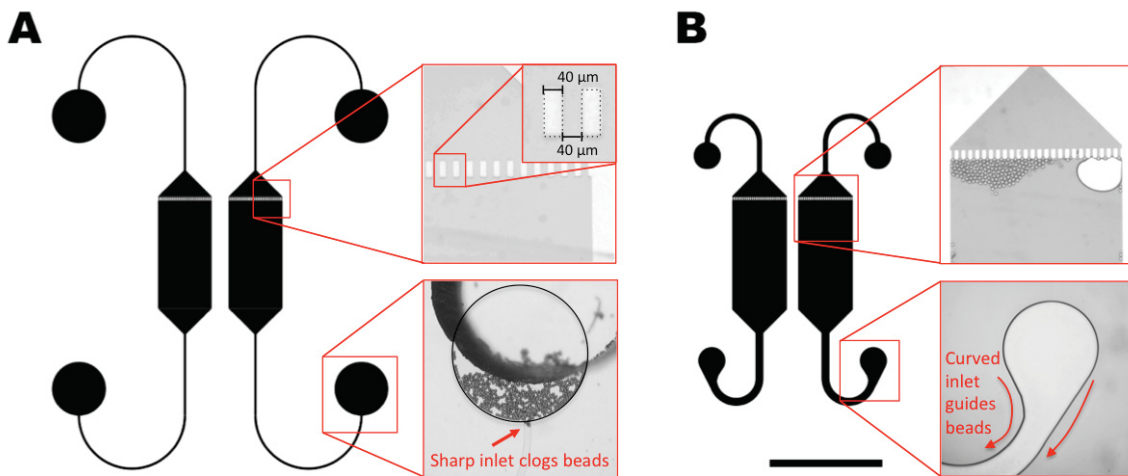


Figure 19: Microfluidic bead trap sieve designs. Each device consists of two chambers to run the experiment (antibody coated beads) and negative control (BSA coated beads) simultaneously. A) Original bead trap design with 40 μm sieves. Inset shows problematic bead clogging at inlet channels. B) Second version of the bead trap with larger, curved inlet channels to avoid bead clogging, and 37 μm sieves. Inset shows beads being trapped at the sieves. Scale bar shows 2 mm.

A 1% suspension of beads was packed into the chambers with high efficiency and reproducible packing (Fig. 20). On each PDMS device, two chambers were present; one chamber was packed with anti-O157:H7 coated beads, and the adjacent chamber was packed with BSA coated beads as a negative control. Both chambers were run with identical assay reagents simultaneously to directly compare capture versus control.

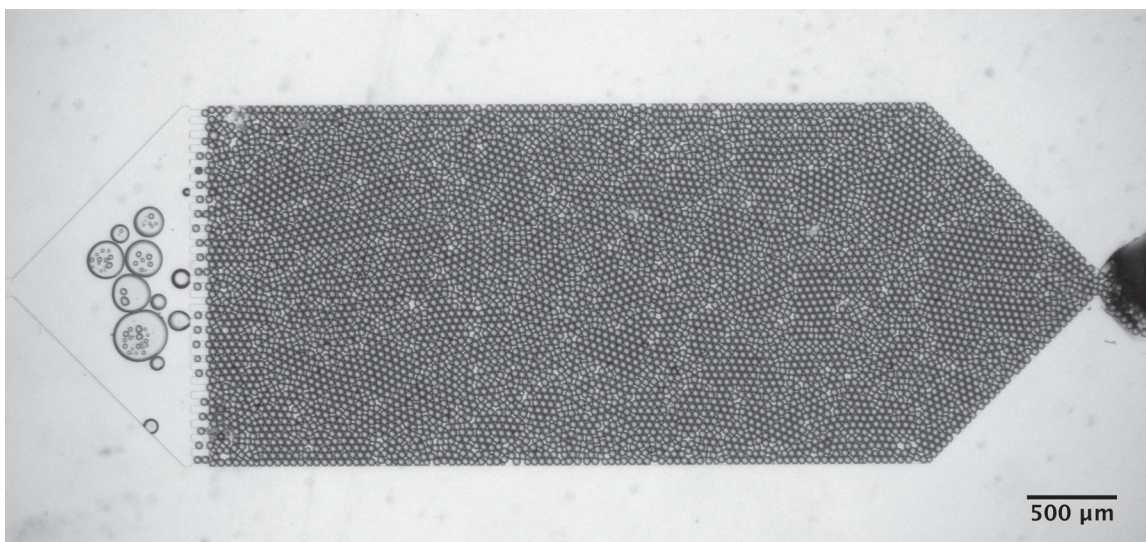


Figure 20: Microfluidic bead trap packed with PMMA microbeads. Microbeads 38-45 μm in diameter are trapped in place by 37 μm sieve channels, producing a packed bed of microbeads roughly 100 μm in depth.

PMMA beads were carboxylated through acid catalyzed hydrolysis and immobilized to anti-O157:H7 antibodies or BSA through EDC/NHS coupling (Section 2.4). To test the efficacy of protein coupling to beads, fluorescent IgG Alexa Fluor® 488 (Life Technologies) was coupled to EDC/NHS activated beads at 0.4 mg/ml (Fig. 21A). As a negative control, a second set of beads was first blocked with 2% Bovine Serum Albumin (BSA) for 2 h, followed by incubation with the same concentration of Alexa Fluor® 488 for 2 h to test blocking (Fig. 21B).

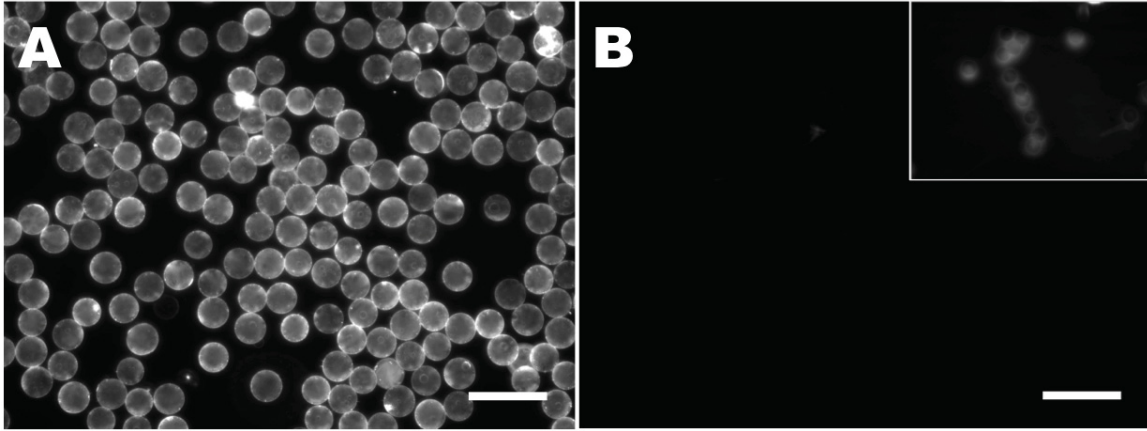


Figure 21: Fluorescent antibody immobilization on carboxylated PMMA microbeads. A) Alexa Fluor® 488 IgG immobilized to carboxylated PMMA microbeads through EDC/NHS coupling compared (1 s exposure), B) negative control, microbeads blocked with BSA and incubation with Alexa Fluor® 488 (1 s exposure). Inset in B) shows weak fluorescent signal at 10 s exposure, verifying the presence of microbeads. Scale bars show 100 μm .

EDC/NHS coupling was shown to be an effective method to immobilize antibodies on microbeads carboxylated through acid catalyzed hydrolysis with good uniformity. EDC/NHS activated beads coupled with 2% BSA were shown to be effective in blocking the surface against Alexa Fluor® 488. These conditions were used to link *anti*-O157:H7 antibodies to beads for bacteria capture, while beads blocked with BSA were used as a negative control. Anti-O157:H7 coated beads were also blocked with 2% BSA for 2 h following antibody coupling to prevent non-specific binding of *E. coli*.

3.4.2 *E. coli* Capture in Bead Traps

Effective capture of *E. coli* in the microfluidic bead trap was demonstrated by passing 1 ml of *E. coli* O157:H7 (10^6 cfu/ml) stained with SYTO® 9 through bead traps packed with antibody immobilized beads (and BSA blocked beads) at 0.05 ml/min, followed by rinsing with 1 ml of PBST (PBS with 0.05% Tween-20). Bead traps were then imaged by fluorescent microscopy. *E. coli* were captured in high density on

antibody-coated beads (Fig. 22A) while very little non-specific binding was observed on blocked beads (Fig. 22B).

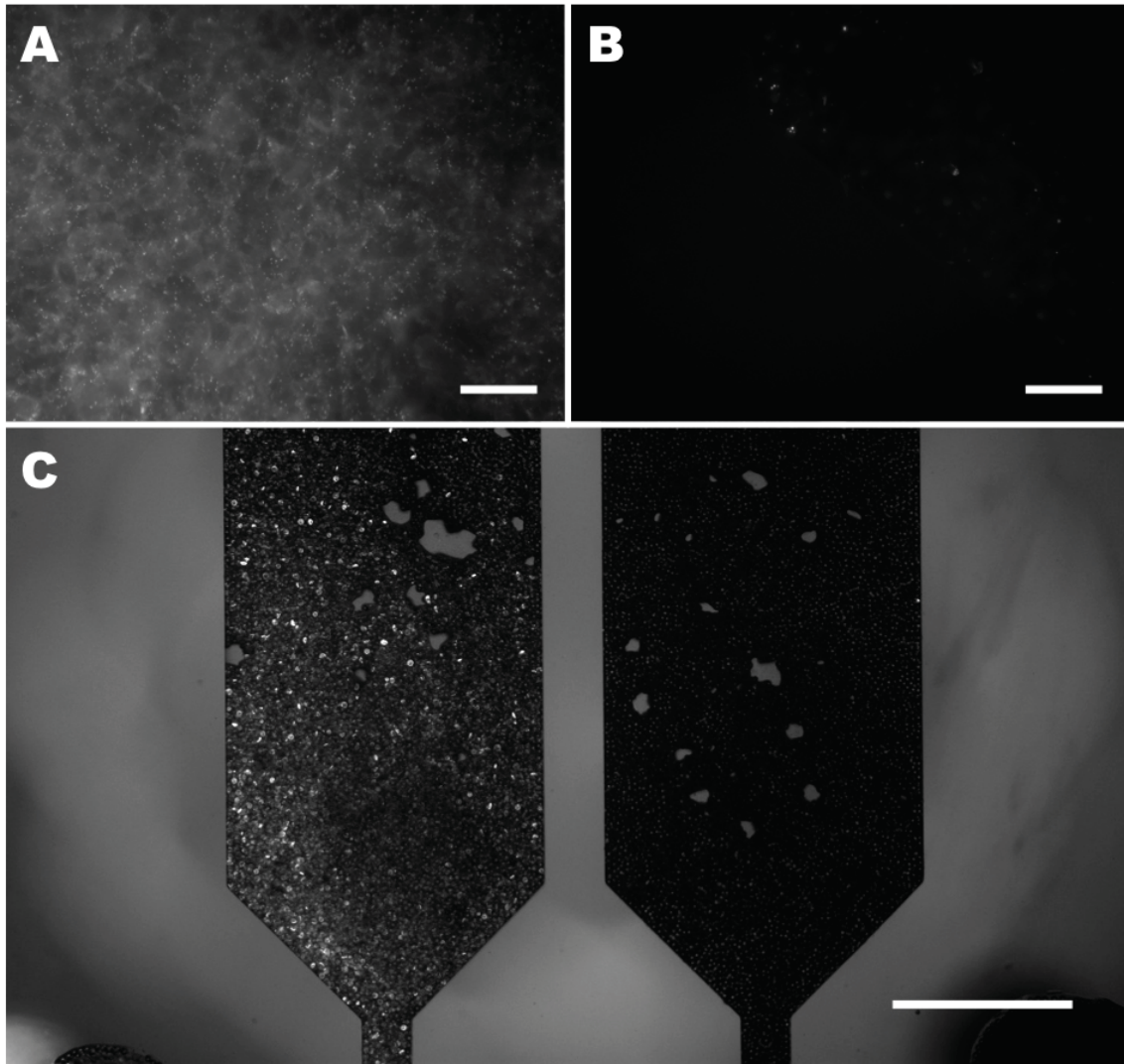


Figure 22: Anti-O157:H7 antibody coated PMMA beads capture *E. coli* O157:H7 in a microfluidic bead trap. A) *E. coli* O157:H7 stained with SYTO® 9 are captured on antibody coated beads versus B) a negative control of BSA coated beads. Scale bars show 100 μm . C) Test (left) and adjacent negative control (right) bead chambers. Scale bar shows 1 mm.

Captured *E. coli* on beads facing the objective could be identified as bacteria cells. However, the fluorescence of cells throughout the packed bed was diffused,

contributing to a net fluorescent intensity of the test chamber, compared to an absence of signal in the negative control. When cells are captured in sufficient number to provide a net fluorescent intensity, this is not problematic. However, for sensitive detection, the microbeads produce spherical aberrations in imaging, and diffuse the fluorescent signal from single cells, making it challenging to identify particles. A similar challenge is present with silver enhanced bacteria, where it becomes challenging to image a dark particle amongst a packed bed of microbeads. Therefore, a strategy to match the refractive index of the microbeads with the surrounding medium was investigated.

3.4.3 Refractive Index Matching of Microbeads

To be able to image silver amplified bacteria cells amongst a packed bed of microbeads, a refractive index matching protocol was developed. By matching the refractive index (n_D) of the microbeads with the surrounding media, the packed bed should theoretically become optically transparent and vanish. Only the dark, silver enhanced particles captured on the surface of microbeads would remain visible, allowing them to be easily picked out and counted.

Originally, polystyrene beads were considered for the microbead trap, given they are readily available with functionalized surfaces for antibody immobilization at low cost. However, the refractive index of polystyrene ($n_D = 1.55-1.59$), and in fact most polymers, is high when compared with liquids such as water ($n_D = 1.33$). For the refractive index matching approach to work appropriately, the microbead material and media must be very closely matched. Oils, such as silicon oil ($n_D = 1.33-1.58$) generally have higher refractive index than aqueous solutions. However, using oils is problematic when the assay is conducted in aqueous phase, as the immiscibility of the oil in water prevents

effective coating of the microbeads; the water phase could not be effectively displaced by oil without trapping microdroplets of water. Other liquids with high refractive index ($n_D > 1.58$) are rare, and most often toxic organic solvents, such as Aniline, Bromoform, Iodobenzene, Quinoline, and Carbon disulfide (Wiederseiner, Andreini, Epely-Chauvin, & Ancy, 2010).

PMMA beads were selected for both their optical transparency and their low refractive index ($n_D = 1.49$) compared to other polymers used for the fabrication of microbeads. A select few aqueous solutions possess refractive indices that (at their maximum) can match that of PMMA, thereby avoiding the problems posed by matching with oils or other toxic solvents.

Matching the refractive index and density of microbeads with the surrounding fluid is of interest for studies in the field of fluid dynamics for the use of techniques such as Particle Image Velocimetry and Laser Doppler Velocimetry, where turbidity caused by concentrated particle suspensions has been a major limitation (Wiederseiner et al., 2010). For refractive index matching with PMMA, concentrated solutions of thiocyanate salts in water have been shown capable of increasing the refractive index significantly, while maintaining a low viscosity (Bailey & Yoda, 2003). Moreover, these solutions are non-toxic, unlike most high refractive index liquids. A solution of 64% (w/w) ammonium thiocyanate (NH_4SCN) in water was selected for its ability to reach a refractive index up to 1.50 while maintaining low viscosity (~ 4.99 cP) (Budwig, 1994). 0.64 g of NH_4SCN was dissolved in 360 μl of Milli-Q water by vortexing. The solution was loaded into a 1 ml syringe, and pumped into bead chambers packed with PMMA beads in water. The ammonium thiocyanate solution was able to match the refractive index of the PMMA

microbeads, and closely match the PDMS, making the packed bed of beads optically transparent and appear to vanish within seconds (Fig. 23).

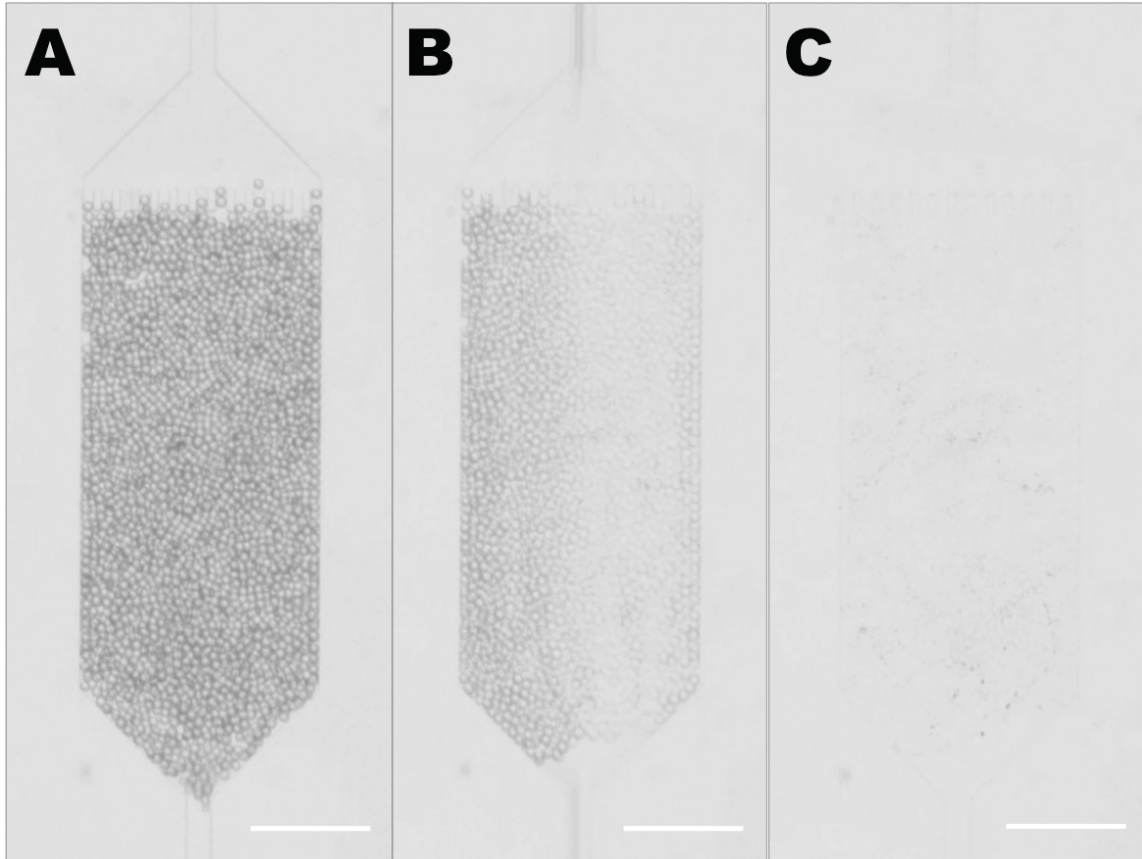


Figure 23: Time course micrograph of refractive index matching PMMA beads with 64% aqueous ammonium thiocyanate. PMMA beads in water at A) 0 s, being flushed with 64% aqueous NH_4SCN at B) 4 s and C) 8 s. Upon refractive index matching, the beads become virtually invisible. Scale bar shows 1 mm.

3.4.4 Silver Enhancement Assay in Microbead Traps

Following demonstration that the refractive index matching protocol was effective in eliminating imaging artifacts from the packed bed of microbeads, the silver enhancement assay was conducted within the bead chambers. As before, PMMA beads immobilized to anti-O157:H7 were packed into one chamber, and compared with a

negative control of BSA coated beads in the adjacent chamber. A 1 ml culture of *E. coli* O157:H7 (10^4 cfu/ml) was flown through the bead traps at a rate of 0.05 ml/min, followed by rinsing with 0.5 ml of PBS. Next, 1 ml of detection antibodies (20 μ g/ml) immediately followed by 1 ml of streptavidin nanogold (100 \times dilution), were passed through the device at 0.05 ml/min, followed by rinsing with 0.5 ml of DI water. Finally, silver enhancement reagents were pumped through at 0.05 ml/min for 5 min, immediately followed by washing with 1 ml of DI water.

The bead chambers were imaged by dark field microscopy before and after refractive index matching with 64% ammonium thiocyanate (Fig. 24). Before refractive index matching, the capture antibody beads showed an inhomogeneous distribution of reflective regions (Fig. 24A), compared to the negative control where primarily only the edges of microbeads were observed, which is characteristic of the dark field microscopy approach (Fig. 24B). Following the addition of ammonium thiocyanate, what appears to be silver coated bacteria, and clusters of bacteria became apparent (Fig. 24C). Those particles within the focal plane appeared to be the size and morphology of *E. coli*. However, regions out of the focal plane appeared as diffuse regions of reflected light. By adjusting the focal plane, these diffuse regions appear as clustered cells. This is not a challenge with the refractive index matching approach, but instead a limited depth of focus. This problem could be resolved by imaging at different depths of focus to identify cells, or alternatively using a chamber of less depth with smaller beads. On the negative control, very few reflective particles were observed (Fig. 24D), suggesting bacteria was not captured, and the non-specific binding or physical trapping of *E. coli* O157:H7 was considerably low. Given that the silver amplification happens only on bacteria coated by

detection antibodies, these are presumably *E. coli* O157:H7 as well. Cells not possessing the surface antigens targeted by the detection bodies would not be silver enhanced, and would not be visible.

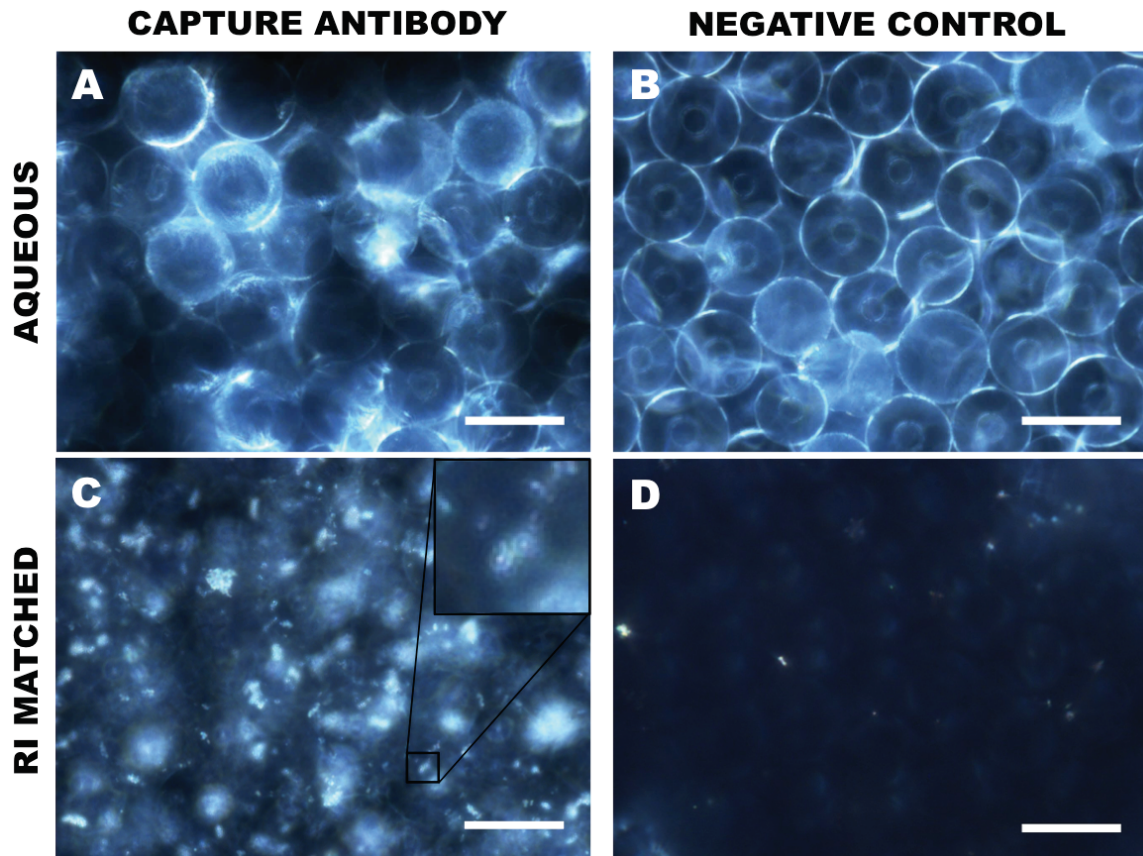


Figure 24: Dark field images of silver enhanced *E. coli* O157:H7 is the microbead trap using refractive index matching. A) Capture of *E. coli* on beads coated with anti-O157:H7 versus B) a negative control of BSA coated beads. Microbeads are clearly visible, and silver enhanced bacteria cannot be observed. C) Silver enhanced bacteria captured by antibody-coated beads becomes visible following refractive index matching with 64% aqueous ammonium thiocyanate. Inset shows what appear to be individual silver coated *E. coli* O157:H7. D) Negative control following refractive index matching shows low capture of *E. coli* O157:H7. Scale bars show 50 μm .

Using this approach, a concentration of 10^4 cfu/ml of *E. coli* O157:H7 was detectable with a sample volume of 1 ml, significantly improving the sensitivity of $\sim 10^7$

cfu/ml obtained on flat glass. This can be attributed to an increase in surface area, and increased interactions of bacteria with the surface they pass through the packed bed, but also from the overall number of cells contained in a 1 ml volume of culture. While larger sample volumes could feasibly be used, this would require either a higher flow rate (possibly reducing bacteria capture efficiency) or an increased time to pass the larger sample. Handling large liquid volumes also negates from the potential use of the approach as a rapid, point-of-care diagnostic test where small sample volumes are preferred. Nevertheless, it is feasible the sensitivity can be further improved, and the sample volume of bacteria culture reduced.

These results are preliminary, but they demonstrate that it is possible to capture and image individual bacteria using the silver enhancement assay on beads with refractive index matching. It is necessary to improve the imaging technique to achieve the desired particle counting at low concentrations of bacteria, which will be the focus of future work (Section 4.2). Future work will optimize silver enhancement assay within the packed bed to increase sensitivity, and produce a standard curve to estimate a limit of detection. Also, the imaging approach which is currently limited by the depth of focus will be further improved, possibly using post-image reconstruction and deconvolution approaches, so that individual particles of silver enhanced bacteria dispersed throughout the depth of the packed bed can be counted to estimate the sample concentration.

4.0 Conclusion

A novel silver enhancement-based sandwich assay has been presented here for the detection of pathogenic bacteria, as demonstrated by a proof-of-concept assay for *E. coli*

O157:H7. The approach is rapid and can go from sample to answer in less than 2 h. The silver enhancement assay eliminates the need for fluorescent microscopy, and, given that silver-coated cells can be imaged at low magnification, inexpensive imaging equipment could be used to enumerate cells and estimate concentration. Since individual bacterium could feasibly be counted using this approach, it is also possible that with future optimization of sensitivity, bacterial diagnostics could be completed without the need for amplification steps. The silver enhancement assay presented here is advantageous over other contrast enhancement techniques, such as crystal violet staining which do not provide strain specificity. Crystal violet staining only distinguishes between Gram positive versus Gram negative bacteria, and must use the morphology of cells to further classify strain. The silver enhancement assay provides specificity through the use of strain specific antibodies to only capture and amplify the desired target. It is believed that the strategies presented here can be widely applied to other pathogenic strains of bacteria by changing the binders for capture and detection to strain specific surface antigens.

4.1 Summary

Bacteriophage and antibodies were evaluated as binders for the capture of *E. coli* from the sample. The binding conditions were optimized on various surfaces for covalent linkage (epoxy, APTES/glutaraldehyde, Xenobind®) using a microarray platform to vary pH, concentration, and printing buffer simultaneously. T4 bacteriophage were found to be effective in capturing *E. coli* K-12 with low background when blocking with BSA. Using a high titer of phage (10^{12} pfu/ml) suspended in 50% glycerol at pH 9.0, optimal results were achieved on Xenobind® reactive aldehyde-coated glass. Antibodies were examined as an alternative to phage for the capture of *E. coli*. Antibodies offer some benefits over

phage, given their wide availability, ease of use, and lower shear sensitivity as observed here with tailed phage. Moreover, antibodies can often be readily produced for a target pathogen. Optimal conditions for the immobilization of antibodies were found on reactive aldehyde surfaces (APTES/glutaraldehyde and Xenobind®) at pH 9.0 using a printing buffer of 2M betaine + 25% 1,3-butanediol. Using BSA for blocking, high density capture with low non-specific binding was demonstrated.

Antibodies were chosen to demonstrate a proof-of-concept silver enhancement assay for detection of *E. coli* O157:H7 on Xenobind glass. *E. coli* captured by immobilized anti-O157:H7 antibodies were coated with biotinylated anti-*E. coli* detection antibodies. Streptavidin-nanogold was introduced to bind to detection antibodies, and catalyze the local reduction of silver from silver enhancement reagents on the cell surface. Cells became visible under dark field microscopy as bright metallic particles and could be enumerated with particle counting algorithms. On flat glass, a sensitivity of roughly 10^7 cfu/ml was demonstrated.

To improve sensitivity, a packed bed of PMMA microbeads in a microfluidic bead trap was proposed. A bead trap using sieves of channels slightly smaller than the diameter of microbeads was designed and fabricated in PDMS. PMMA microbeads were selected based on their transparency and low refractive index ($n_D = 1.49$) compared with other microbead polymers. This allowed for an aqueous refractive index matching fluid of 64% ammonium thiocyanate ($n_D = 1.49$) to be used to eliminate the background variations in intensity caused by the packed bed. Within the packed bed, preliminary results show silver coated cells can be detected at 10^4 cfu/ml. While this result is promising, future work on optimizing the imaging approach to combat challenges with

the depth of field and performing replicate experiments for estimations of sensitivity must be completed to make this a viable approach for the detection of pathogenic bacteria.

4.2 Future Work

Future work should focus on improving the imaging of silver enhanced cells within the packed bed, and estimating the limit of detection through the generation of a standard curve. Conventional microscopy shows only a lateral plane of focus, meaning that the depth of field limits effective imaging to thin samples. Here, many silver coated cells distributed throughout the packed bed are out of the focal plane, and appear as diffuse areas under dark field microscopy. To address this challenge, methods of optical sectioning, where images are taken at each focal plane (and out-of-focus regions are excluded) could be used to better enumerate particles. This could be achieved in one of three ways: i) using solely optical methods where out of focus light is filtered out (such as with scanning point confocal microscopy), ii) using computational methods (such as deconvolution microscopy) to reconstruct out-of-focus light, or iii) using patterned light (such as structured illumination microscopy) to encode additional information within images that can be used with computational methods in post-processing to reconstruct the image (Langhorst, Schaffer, & Goetze, 2009). The most commonly used technique for imaging 3D samples is confocal microscopy, however this typically requires expensive imaging equipment to conduct. Structured illumination microscopy has recently become an attractive alternative to confocal microscopy given its ease of use, lower-cost and theoretically unlimited resolution (Gustafsson, 2005; Langhorst et al., 2009). Structured illumination microscopy provides one approach that could be investigated as a simple means to image the 3D distribution of silver enhanced cells within the packed bed.

Once a suitable imaging approach is optimized, an estimation of the sensitivity than can be achieved using this approach can be determined. At high concentrations, it is likely that a net grayscale value (from the high density of silver coated cells) at low magnification would be sufficient to estimate concentration. At a threshold concentration with low cell count, detection would switch from a net intensity approach to a particle counting approach to enumerate individual bacteria, potentially offering high sensitivity. The threshold concentration to switch to particle counting should be further investigated to determine the range of sample concentrations suitable for detection.

Once the detection scheme has been optimized, this sensing approach should be applied to other pathogens, such as highly prevalent MRSA infections, to demonstrate its application to the detection of hospital acquired infections. MRSA is most often detected through real time PCR, using probes for the *mecA* and *femA* genes. The *mecA* gene encodes for the mutant penicillin binding protein PBP2a responsible for antibiotic resistance (Ubukata et al., 1989), while the *femA* gene verifies the strain as *S. aureus* (Sabet, Subramaniam, Navaratnam, & Sekaran, 2007). Latex agglutination tests that use microbeads coated with anti-PBP2a have been shown to be a simple and effective means to detect MRSA, given a high enough culture concentration (van Leeuwen, van Pelt, Luijendijk, Verbrugh, & Goessens, 1999). Since PBP2a is expressed on the surface of MRSA, antibodies against PBP2a could provide specificity for methicillin resistance, while anti-*S. aureus* detection antibodies could confirm the strain. This detection approach would therefore be analogous to the PCR detection method, but by using the proteins expressed rather than the genes that encode them.

The detection of bacterial pathogens using this approach should also be tested in complex sample matrices. Real-world samples generally contain debris or interferents that may affect the capture and detection of cells. For HAIs, samples such as blood, tissue or mucus from a nasal swab or nasopharyngeal aspirate are typically used for diagnosis of bacterial infection. Similarly, food samples are generally ground into a slurry and incubated to amplify the number of bacteria. These complex sample matrices effect the diffusion of bacteria cells and the efficacy of antibodies in binding to the target. The device will need to be characterized in working with such samples. Sample preparation may become an important step and filtering the sample to remove large debris is likely needed. Moreover, testing for false positives and negatives in real world samples will be an important step in characterizing such a diagnostic test, and the appropriate controls should be integrated in the device.

Ultimately, the goal of this work is to develop rapid, low-cost approaches for the detection of pathogenic bacteria on-site or at the POC. While the proof-of-concept approach presented here demonstrates one method that could be used to achieve such goals, it would still require the appropriate equipment and trained personnel to complete. However, it is feasible that the assay could be completed autonomously within an integrated biosensor. Using self-powered, pre-programmed microfluidic operations, as in capillarics (Safavieh & Juncker, 2013), the necessary reagents to complete the assay could be pre-loaded within a microfluidic chip and triggered to release in sequential order, completing the assay without the need for external equipment or a power supply. This would allow extreme ease of use in a low-cost, disposable biosensor to rapidly detect pathogenic bacteria in many different environments.

Abbreviations

APTES	(3-Aminopropyl)triethoxysilane
BSA	Bovine Serum Albumin
cfu	Colony-Forming Unit
CPS	Capsular Polysaccharide (layer)
CTC	Circulating Tumor Cell
DI	De-Ionized (water)
DSLR	Digital Single Reflex Lens (camera)
<i>E. coli</i>	<i>Escherichia coli</i>
EDC	1-Ethyl-3-(3-dimethylaminopropyl)carbodiimide
EHEC	Enterohaemorrhagic <i>E. coli</i>
ELISA	Enzyme Linked Immunosorbent Assay
GFP	Green Fluorescent Protein
HAI	Hospital Acquired Infection
IgG	Immunoglobulin G
K-12	Laboratory <i>E. coli</i> strain
LB	Lysogeny Broth
LPS	Lipopolysaccharide (layer)
MES	2-(<i>N</i> -morpholino)ethanesulfonic Buffer (pH ~5.5)
MRSA	Methicillin-resistant <i>Staphylococcus aureus</i>
MW	Molecular Weight
n_D	Refractive Index
NHS	N-Hydroxysuccinimide
NMWL	Nominal Molecular Weight Limit
OmpC	Outer Membrane Protein C
PBP-2a	Penicillin Binding Protein 2a
PBS	Phosphate Buffered Saline (pH ~7.5)
PBST	Phosphate Buffered Saline with Tween-20 (0.05%)
PCR	Polymerase Chain Reaction
PDMS	Polydimethylsiloxane
PEG	Polyethylene glycol
pfu	Plaque-Forming Unit
phage	Bacteriophage
PLL	Poly-L-Lysine
PMMA	Poly(methyl methacrylate)
POC	Point-of-Care
PS	Polystyrene
SMG	Phage Storage Buffer (NaCl, MgSO ₄ , HCl, Gelatin)
STEC	Shiga-Toxin producing <i>E. coli</i>
SU-8	1-Methoxy-2-propanol acetate (epoxy-based photoresist)
SYTO® 9	Green Fluorescent Nucleic Acid Stain
TBS	Tris Buffered Saline
VTEC	Verotoxin producing <i>E. coli</i>

References

- Ahmad, F., & Hashsham, S. A. (2012). Miniaturized nucleic acid amplification systems for rapid and point-of-care diagnostics: a review. *Anal Chim Acta*, 733, 1-15.
- Albert, H., Manabe, Y., Lukyamuzi, G., Ademun, P., Mukkada, S., Nyesiga, B., . . . Perkins, M. D. (2010). Performance of three LED-based fluorescence microscopy systems for detection of tuberculosis in Uganda. *PLoS One*, 5(12), e15206.
- Almeida, R. J., Hickman-Brenner, F. W., Sowers, E. G., Puhr, N. D., Farmer, J. J., 3rd, & Wachsmuth, I. K. (1990). Comparison of a latex agglutination assay and an enzyme-linked immunosorbent assay for detecting cholera toxin. *J Clin Microbiol*, 28(1), 128-130.
- Baccar, H., Mejri, M. B., Hafaiedh, I., Ktari, T., Aouni, M., & Abdelghani, A. (2010). Surface plasmon resonance immunosensor for bacteria detection. *Talanta*, 82(2), 810-814.
- Bailey, B. C., & Yoda, M. (2003). An aqueous low-viscosity density- and refractive index-matched suspension system. *Experiments in Fluids*, 35(1), 1-3.
- Ball, H. J., Finlay, D., Burns, L., & Mackie, D. P. (1994). Application of Monoclonal Antibody-Based Sandwich Elisas to Detect Verotoxins in Cattle Feces. *Research in Veterinary Science*, 57(2), 225-232.
- Bergeron, S., Laforte, V., Lo, P. S., Li, H., & Juncker, D. (2014). *Low-Evaporation Additives for Printing Antibody Microarrays using Silicon Quill Pins*. . Paper presented at the Canadian National Proteomics Network, 6th Symposium, Montreal, Quebec, Canada
- Bernard, A., Renault, J. P., Michel, B., Bosshard, H. R., & Delamarche, E. (2000). Microcontact printing of proteins. *Advanced Materials*, 12(14), 1067-1070.
- Birch, J. R., & Racher, A. J. (2006). Antibody production. *Adv Drug Deliv Rev*, 58(5-6), 671-685.
- Blok, H. E., Troelstra, A., Kamp-Hopmans, T. E., Gigengack-Baars, A. C., Vandenbroucke-Grauls, C. M., Weersink, A. J., . . . Mascini, E. M. (2003). Role of healthcare workers in outbreaks of methicillin-resistant *Staphylococcus aureus*: a 10-year evaluation from a Dutch university hospital. *Infect Control Hosp Epidemiol*, 24(9), 679-685.
- Bonnet, M., Gagnidze, L., Githui, W., Guerin, P. J., Bonte, L., Varaine, F., & Ramsay, A. (2011). Performance of LED-based fluorescence microscopy to diagnose tuberculosis in a peripheral health centre in Nairobi. *PLoS One*, 6(2), e17214.
- Breadmore, M. C., Wolfe, K. A., Arcibal, I. G., Leung, W. K., Dickson, D., Giordano, B. C., . . . Landers, J. P. (2003). Microchip-based purification of DNA from biological samples. *Anal Chem*, 75(8), 1880-1886.
- Brooks, B. W., Devenish, J., Lutze-Wallace, C. L., Milnes, D., Robertson, R. H., & Berlie-Surujballi, G. (2004). Evaluation of a monoclonal antibody-based enzyme-linked immunosorbent assay for detection of *Campylobacter fetus* in bovine preputial washing and vaginal mucus samples. *Vet Microbiol*, 103(1-2), 77-84.
- Budwig, R. (1994). Refractive-Index Matching Methods for Liquid Flow Investigations. *Experiments in Fluids*, 17(5), 350-355.
- Buzby, J. C., & Roberts, T. (2009). The economics of enteric infections: human foodborne disease costs. *Gastroenterology*, 136(6), 1851-1862.

- Cady, N. C., Stelick, S., Kunnavakkam, M. V., & Batt, C. A. (2005). Real-time PCR detection of *Listeria monocytogenes* using an integrated microfluidics platform. *Sensors and Actuators B: Chemical*, *107*(1), 332-341.
- Carlton, R. M. (1999). Phage therapy: past history and future prospects. *Arch Immunol Ther Exp (Warsz)*, *47*(5), 267-274.
- Chin, C. D., Laksanasopin, T., Cheung, Y. K., Steinmiller, D., Linder, V., Parsa, H., . . . Sia, S. K. (2011). Microfluidics-based diagnostics of infectious diseases in the developing world. *Nat Med*, *17*(8), 1015-1019.
- Clokier, M. R. J., & Kropinski, A. M. (2009). Enumeration of Bacteriophages by Double Agar Overlay Plaque Assay. *501*.
- Cosgrove, S. E., Sakoulas, G., Perencevich, E. N., Schwaber, M. J., Karchmer, A. W., & Carmeli, Y. (2003). Comparison of mortality associated with methicillin-resistant and methicillin-susceptible *Staphylococcus aureus* bacteremia: a meta-analysis. *Clin Infect Dis*, *36*(1), 53-59.
- Dansch, G., & Rytter Norgaard, J. O. (1985). Ultrastructural autometallography: a method for silver amplification of catalytic metals. *Journal of Histochemistry & Cytochemistry*, *33*(7), 706-710.
- Deegan, R. D., Bakajin, O., Dupont, T. F., Huber, G., Nagel, S. R., & Witten, T. A. (1997). Capillary flow as the cause of ring stains from dried liquid drops. *Nature*, *389*(6653), 827-829.
- DeLeo, F. R., Otto, M., Kreiswirth, B. N., & Chambers, H. F. (2010). Community-associated methicillin-resistant *Staphylococcus aureus*. *Lancet*, *375*(9725), 1557-1568.
- Donlan, R. M. (2009). Preventing biofilms of clinically relevant organisms using bacteriophage. *Trends Microbiol*, *17*(2), 66-72.
- Duckworth, D. H. (1970). Biological activity of bacteriophage ghosts and "take-over" of host functions by bacteriophage. *Bacteriol Rev*, *34*(3), 344-363.
- Edgar, R., McKinsty, M., Hwang, J., Oppenheim, A. B., Fekete, R. A., Giulian, G., . . . Adhya, S. (2006). High-sensitivity bacterial detection using biotin-tagged phage and quantum-dot nanocomplexes. *Proc Natl Acad Sci U S A*, *103*(13), 4841-4845.
- Esposito, D., Fitzmaurice, W. P., Benjamin, R. C., Goodman, S. D., Waldman, A. S., & Scocca, J. J. (1996). The complete nucleotide sequence of bacteriophage HP1 DNA. *Nucleic Acids Res*, *24*(12), 2360-2368.
- Foudeh, A. M., Fatanat Didar, T., Veres, T., & Tabrizian, M. (2012). Microfluidic designs and techniques using lab-on-a-chip devices for pathogen detection for point-of-care diagnostics. *Lab Chip*, *12*(18), 3249-3266.
- Gau, J. J., Lan, E. H., Dunn, B., Ho, C. M., & Woo, J. C. S. (2001). A MEMS based amperometric detector for E-Coli bacteria using self-assembled monolayers. *Biosens Bioelectron*, *16*(9-12), 745-755.
- Gracias, K. S., & McKillip, J. L. (2004). A review of conventional detection and enumeration methods for pathogenic bacteria in food. *Can J Microbiol*, *50*(11), 883-890.
- Guan, X., Zhang, H. J., Bi, Y. N., Zhang, L., & Hao, D. L. (2010). Rapid detection of pathogens using antibody-coated microbeads with bioluminescence in microfluidic chips. *Biomed Microdevices*, *12*(4), 683-691.

- Gustafsson, M. G. (2005). Nonlinear structured-illumination microscopy: wide-field fluorescence imaging with theoretically unlimited resolution. *Proc Natl Acad Sci U S A*, *102*(37), 13081-13086.
- Hanly, W. C., Artwohl, J. E., & Bennett, B. T. (1995). Review of Polyclonal Antibody Production Procedures in Mammals and Poultry. *ILAR J*, *37*(3), 93-118.
- Ivnitski, D., Abdel-Hamid, I., Atanasov, P., & Wilkins, E. (1999). Biosensors for detection of pathogenic bacteria. *Biosens Bioelectron*, *14*(7), 599-624.
- Jackson, B. R., Griffin, P. M., Cole, D., Walsh, K. A., & Chai, S. J. (2013). Outbreak-associated *Salmonella enterica* serotypes and food Commodities, United States, 1998-2008. *Emerg Infect Dis*, *19*(8), 1239-1244.
- Kaigala, G. V., Hoang, V. N., Stickel, A., Lauzon, J., Manage, D., Pilarski, L. M., & Backhouse, C. J. (2008). An inexpensive and portable microchip-based platform for integrated RT-PCR and capillary electrophoresis. *Analyst*, *133*(3), 331-338.
- Kaper, J. B., Nataro, J. P., & Mobley, H. L. (2004). Pathogenic *Escherichia coli*. *Nat Rev Microbiol*, *2*(2), 123-140.
- Koskella, B., & Meaden, S. (2013). Understanding bacteriophage specificity in natural microbial communities. *Viruses*, *5*(3), 806-823.
- Krueger, A. P., Ritter, R. C., & Smith, S. P. (1929). The Electrical Charge of Bacteriophage. *J Exp Med*, *50*(6), 739-746.
- Langhorst, M. F., Schaffer, J., & Goetze, B. (2009). Structure brings clarity: structured illumination microscopy in cell biology. *Biotechnol J*, *4*(6), 858-865.
- Lazcka, O., Del Campo, F. J., & Munoz, F. X. (2007). Pathogen detection: a perspective of traditional methods and biosensors. *Biosens Bioelectron*, *22*(7), 1205-1217.
- Lillehoj, P. B., Kaplan, C. W., He, J., Shi, W., & Ho, C. M. (2014). Rapid, electrical impedance detection of bacterial pathogens using immobilized antimicrobial peptides. *J Lab Autom*, *19*(1), 42-49.
- Liu, P., Li, X., Greenspoon, S. A., Scherer, J. R., & Mathies, R. A. (2011). Integrated DNA purification, PCR, sample cleanup, and capillary electrophoresis microchip for forensic human identification. *Lab Chip*, *11*(6), 1041-1048.
- MacBeath, G. (2002). Protein microarrays and proteomics. *Nat Genet*, *32 Suppl*, 526-532.
- Mairhofer, J., Roppert, K., & Ertl, P. (2009). Microfluidic systems for pathogen sensing: a review. *Sensors (Basel)*, *9*(6), 4804-4823.
- Mao, X., Yang, L., Su, X. L., & Li, Y. (2006). A nanoparticle amplification based quartz crystal microbalance DNA sensor for detection of *Escherichia coli* O157:H7. *Biosens Bioelectron*, *21*(7), 1178-1185.
- Merker, B. (1983). Silver staining of cell bodies by means of physical development. *J Neurosci Methods*, *9*(3), 235-241.
- Nagrath, S., Sequist, L. V., Maheswaran, S., Bell, D. W., Irimia, D., Ulkus, L., . . . Toner, M. (2007). Isolation of rare circulating tumour cells in cancer patients by microchip technology. *Nature*, *450*(7173), 1235-1239.
- Nam, J. M., Thaxton, C. S., & Mirkin, C. A. (2003). Nanoparticle-based bio-bar codes for the ultrasensitive detection of proteins. *Science*, *301*(5641), 1884-1886.
- NIDD. (2008). A Battle We Can Win: Reducing Healthcare Associated Infections by 50%: National Infectious Diseases Day.

- Oliveira, I. C., Almeida, R. C. C., Hofer, E., & Almeida, P. F. (2012). Bacteriophage Amplification Assay for Detection of *Listeria* Spp. Using Virucidal Laser Treatment. *Brazilian Journal of Microbiology*, 43(3), 1128-1136.
- Olle, E. W., Messamore, J., Deogracias, M. P., McClintock, S. D., Anderson, T. D., & Johnson, K. J. (2005). Comparison of antibody array substrates and the use of glycerol to normalize spot morphology. *Exp Mol Pathol*, 79(3), 206-209.
- Ott, S., Niessner, R., & Seidel, M. (2011). Preparation of epoxy-based macroporous monolithic columns for the fast and efficient immunofiltration of *Staphylococcus aureus*. *J Sep Sci*.
- Papia, G., Louie, M., Tralla, A., Johnson, C., Collins, V., & Simor, A. E. (1999). Screening high-risk patients for methicillin-resistant *Staphylococcus aureus* on admission to the hospital: is it cost effective? *Infect Control Hosp Epidemiol*, 20(7), 473-477.
- Park, S., Zhang, Y., Lin, S., Wang, T. H., & Yang, S. (2011). Advances in microfluidic PCR for point-of-care infectious disease diagnostics. *Biotechnol Adv*, 29(6), 830-839.
- Qiu, J., Zhou, Y., Chen, H., & Lin, J. M. (2009). Immunomagnetic separation and rapid detection of bacteria using bioluminescence and microfluidics. *Talanta*, 79(3), 787-795.
- Rainaldi, G., Calcabrini, A., & Santini, M. T. (1998). Positively charged polymer polylysine-induced cell adhesion molecule redistribution in K562 cells. *J Mater Sci Mater Med*, 9(12), 755-760.
- Reed, D., & Kemmerly, S. A. (2009). Infection control and prevention: a review of hospital-acquired infections and the economic implications. *Ochsner J*, 9(1), 27-31.
- Roper, M. G., Easley, C. J., & Landers, J. P. (2005). Advances in polymerase chain reaction on microfluidic chips. *Anal Chem*, 77(12), 3887-3893.
- Sabet, N. S., Subramaniam, G., Navaratnam, P., & Sekaran, S. D. (2007). Detection of methicillin- and aminoglycoside-resistant genes and simultaneous identification of *S. aureus* using triplex real-time PCR Taqman assay. *J Microbiol Methods*, 68(1), 157-162.
- Safavieh, R., & Juncker, D. (2013). Capillarics: pre-programmed, self-powered microfluidic circuits built from capillary elements. *Lab Chip*, 13(21), 4180-4189.
- Sambrook, J., & Russell, D. W. (2001). *Molecular Cloning: A Laboratory Manual* (3rd ed.). Cold Spring Harbour, NY: Cold Spring Harbour Laboratory Press.
- Sauer-Budge, A. F., Mirer, P., Chatterjee, A., Klapperich, C. M., Chargin, D., & Sharon, A. (2009). Low cost and manufacturable complete microTAS for detecting bacteria. *Lab Chip*, 9(19), 2803-2810.
- Scallan, E., Griffin, P. M., Angulo, F. J., Tauxe, R. V., & Hoekstra, R. M. (2011). Foodborne Illness Acquired in the United States—Unspecified Agents. *Emerging Infectious Diseases*, 17(1), 16-22.
- Scallan, E., Hoekstra, R. M., Angulo, F. J., Tauxe, R. V., Widdowson, M.-A., Roy, S. L., . . . Griffin, P. M. (2011). Foodborne Illness Acquired in the United States—Major Pathogens. *Emerging Infectious Diseases*, 17(1), 7-15.
- Scharnagl, C., Reif, M., & Friedrich, J. (2005). Stability of proteins: temperature, pressure and the role of the solvent. *Biochim Biophys Acta*, 1749(2), 187-213.

- Singh, A., Arutyunov, D., Szymanski, C. M., & Evoy, S. (2012). Bacteriophage based probes for pathogen detection. *Analyst*, 137(15), 3405-3421.
- Su, X. L., & Li, Y. (2005). A QCM immunosensor for Salmonella detection with simultaneous measurements of resonant frequency and motional resistance. *Biosens Bioelectron*, 21(6), 840-848.
- Thomas, M. K., Murray, R., Flockhart, L., Pintar, K., Pollari, F., Fazil, A., . . . Marshall, B. (2013). Estimates of the burden of foodborne illness in Canada for 30 specified pathogens and unspecified agents, circa 2006. *Foodborne Pathog Dis*, 10(7), 639-648.
- Threlfall, E. J. (2002). Antimicrobial drug resistance in Salmonella: problems and perspectives in food- and water-borne infections. *FEMS Microbiol Rev*, 26(2), 141-148.
- Toh, A. G. G., Wang, Z. F., & Ng, S. H. (2008). Fabrication of Embedded Microvalve on PMMA Microfluidic Devices through Surface Functionalization. *Dtip 2008: Symposium on Design, Test, Integration and Packaging of Mems/Moems*, 267-272.
- Ubukata, K., Nonoguchi, R., Matsushashi, M., & Konno, M. (1989). Expression and inducibility in Staphylococcus aureus of the mecA gene, which encodes a methicillin-resistant S. aureus-specific penicillin-binding protein. *J Bacteriol*, 171(5), 2882-2885.
- Van Laere, O., De Wael, L., & De Mey, J. (1985). Immuno gold staining (IGS) and immuno gold silver staining (IGSS) for the identification of the plant pathogenic bacterium Erwinia amylovora (Burrill) Winslow et al. *Histochemistry*, 83(5), 397-399.
- van Leeuwen, W. B., van Pelt, C., Luijendijk, A., Verbrugh, H. A., & Goessens, W. H. (1999). Rapid detection of methicillin resistance in Staphylococcus aureus isolates by the MRSA-screen latex agglutination test. *J Clin Microbiol*, 37(9), 3029-3030.
- Wei, Q., McLeod, E., Qi, H., Wan, Z., Sun, R., & Ozcan, A. (2013). On-chip cytometry using plasmonic nanoparticle enhanced lensfree holography. *Sci Rep*, 3, 1699.
- WHO. (2014). Antimicrobial Resistance - Global Report on Surveillance. France: World Health Organization.
- Wiederseiner, S., Andreini, N., Epely-Chauvin, G., & Ancy, C. (2010). Refractive-index and density matching in concentrated particle suspensions: a review. *Experiments in Fluids*, 50(5), 1183-1206.
- Xing, Y., & Borguet, E. (2007). Specificity and sensitivity of fluorescence labeling of surface species. *Langmuir*, 23(2), 684-688.
- Yeh, C.-H., Chang, Y.-H., Lin, H.-P., Chang, T.-C., & Lin, Y.-C. (2012). A newly developed optical biochip for bacteria detection based on DNA hybridization. *Sensors and Actuators B: Chemical*, 161(1), 1168-1175.
- Yu, F., & Mizushima, S. (1982). Roles of lipopolysaccharide and outer membrane protein OmpC of Escherichia coli K-12 in the receptor function for bacteriophage T4. *J Bacteriol*, 151(2), 718-722.
- Zelada-Guillen, G. A., Bhosale, S. V., Riu, J., & Rius, F. X. (2010). Real-Time Potentiometric Detection of Bacteria in Complex Samples. *Anal Chem*, 82(22), 9254-9260.

- Zeng, Y., & Harrison, D. J. (2007). Self-assembled colloidal arrays as three-dimensional nanofluidic sieves for separation of biomolecules on microchips. *Anal Chem*, 79(6), 2289-2295.
- Zhu, H., Isikman, S. O., Mudanyali, O., Greenbaum, A., & Ozcan, A. (2013). Optical imaging techniques for point-of-care diagnostics. *Lab Chip*, 13(1), 51-67.
- Zhu, H., Sikora, U., & Ozcan, A. (2012). Quantum dot enabled detection of Escherichia coli using a cell-phone. *Analyst*, 137(11), 2541-2544.
- Zourab, M., Elwary, S., & Turner, A. (2008). *Principles of Bacterial Detection: Biosensors, Recognition Receptors and Microsystems*: Springer Science + Business Media.